

One potential issue regarding the applicability of the industry-wide crane data was the inclusion of hard-wired interlock features on the YMP cranes that might not exist at the nuclear power plants or naval installations from which the industry-wide experience resulted. In other instances, there was concern that interlocks included in the design for use in normal operations, on grapples to verify installation or engagement, could be defeated during maintenance actions where bypasses are permitted to move tools or pallets, since a particular grapple interlock is not standard in industry but is unique to YMP. Further, PCSA is not crediting the grapple interlock function and it was considered that having such interlocks in place would not make the estimated failure probability worse. Therefore the estimates from industry-wide data were considered to be reasonable in that they provided experience-based, and perhaps somewhat pessimistic measures of anticipated crane performance.

Estimates were also developed from industry-wide data source information for the likelihood of SFTM drop, collision, and raising the fuel too high but not dropped (for potential personnel exposure considerations). The primary source for this information was NUREG-1774 (Ref. C5.26, Table 4), which provides brief descriptions of SFTM incidents at U.S. nuclear power plants from 1968 through 2002. A separate study (McKenna/Framatome) (Ref. C5.20) was reviewed, which also included SFTM incidents at U.S. nuclear power plants categorized in terms of Human Error, Equipment Failure, or Misload. Some of these were the same incidents included in NUREG-1774 (Ref. C5.26) so care was taken not to double-count any events. Each of the incidents described was reviewed in detail to evaluate their relevance to the failure modes of interest to the study and their applicability to spent fuel transfers. Incidents related to all types of fuel transfers, such as refueling or new fuel receipt, were used to estimate upper bounds (95th percentiles of a lognormal distribution) and to develop the error factor uncertainty information input to SAPHIRE along with the mean value.

It should be noted that events prior to 1985 were removed from consideration since the number of plants in operation (and therefore the number of lifts per year) would significantly differ from that cited in McKenna/Framatome (Ref. C5.20). Also, McKenna/Framatome stated that reporting practices were inconsistent prior to 1985.

The number of fuel movements used as the denominator of the SFTM estimates was based upon information from McKenna/Framatome (Ref. C5.20), which gave 1,198,723 fuel movements for the 15 year study data window, from 1985 through 1999, or a rough estimate of 79,914.87 per year. Since the numerator information from NUREG-1774 (Ref. C5.26) was based upon 17 years of data, from 1985 through 2002, the estimated denominator was calculated for consistency as $79,914.87 \times 17$ or 1,358,553 SFTM lifts.

As a result, several categories of SFTM event estimates were developed, were coded with TYP-FM designators, and were included in the template database for input to SAPHIRE:

SFT-COL	SFTM Collision/Impact	2.9E-06/demand
SFT-DRP	SFTM Load Drop	5.2E-06/demand
SFT-RTH	SFTM Fuel Raised Too High (but not dropped)	7.4E-07/demand

These SFTM incident estimates were combined in the SAPHIRE models with the number of estimated YMP fuel assembly transfers, specifically: 66,188 based on two transfers each of 33,094 assemblies (Ref. C5.7, Table 4, pg. 27).

The results of the industry-wide data search are documented, organized by component type and failure mode, and can be found in the Excel spreadsheet file “YMP Active Comp Database.xls”, located on the CD in Attachment H.

C2 BAYESIAN DATA COMBINATION

The application of industry-wide data sources or expert elicitation introduces uncertainty in the input parameters used in basic events and, ultimately, the quantification of probabilities of event sequences. Uncertainty is a probabilistic concept that is inversely proportional to the amount of knowledge, with less knowledge implying more uncertainty. Bayes’ theorem is a common method of mathematically expressing a decrease in uncertainty gained by an increase in knowledge (for example, knowledge about failure frequency gained by in-field experience).

A typical application of Bayes’ theorem is illustrated as follows: a failure rate for a given component is needed for fault tree (e.g., a fan motor in the heating, ventilation, and air conditioning (HVAC) system). There is no absolute value but there are several data sources for the same kind of fan and/or similar fans that may exhibit considerable variability for many reasons. Applying any or all of the available data introduces uncertainty in the analysis of the reliability of the HVAC system. Bayes’ theorem provides a mechanism for systematically treating the uncertainty and applying λ_j data sources using the following steps:

1. Initially, estimate the failure rate to be within some range with a probability distribution. This is termed the “prior” probability of having a certain value of the failure rate that expresses the state of knowledge before any new information is applied.
2. Characterize the test information, or evidence, in the form of a likelihood function that expresses the probability of observing the number of failures in the given number of trial if the failure rate is a certain value. The evidence comprises observations or test results on the number of failure events that occur in over a certain exposure, operational, or test duration.
3. Update the probability distribution for the failure rate based on the new body of evidence using the mathematical expression of Bayes’ theorem.

The mathematical expression for applying Bayes’ theorem to data analysis is briefly described here. Let λ_j be one failure rate of a set of possible failure rates of the fan motor (component j). Initially, the state of knowledge of the “true value” of λ_j is expressed by the probability distribution $P(\lambda)$, the “prior.” The choice of the analytic or discrete form of the prior distribution is made by the data analyst. Let E be a new body of evidence, e.g., a new set of test data or field observations. The new evidence improves the data analyst’s state of knowledge. The revised, or “updated,” probability distribution for the “true value” of λ_j is represented as $P(\lambda_j|E)$. Bayes’ theorem gives:

$$P(\lambda_j | E) = \frac{P(\lambda_j)L(E | \lambda_j)}{\sum_j P(\lambda_j)P(E | \lambda_j)} \quad (\text{Eq. C-1})$$

In summary, Equation C-1 states that the knowledge of the “updated” probability of λ_j , given the new information E , equals the “prior” probability of λ_j before any new information times the likelihood function, $L(E/\lambda_j)$. The likelihood function expresses the probability of observing the number of failures in the evidence if the failure rate λ_j has a certain value. The likelihood function is defined by the analyst in accordance with the kind of evidence. For time-based failure data, a Poisson model is used for the likelihood function. For demand-based failure data, a binomial model is used. The numerator in Equation C-1 is divided by a normalization factor, which must be such that the sum of the probabilities over the entire set of λ_j equals unity.

There are several approaches for applying Bayes’ theorem to data management and combining data sources, as described in NUREG/CR-6823 (Ref. C5.4). For the YMP PCSA, the method known as “parametric empirical Bayes” was used. This permitted a variety of different sources to be statistically combined and compared, whether the inputs were expressed as the number of failures and exposure time or demands, or as a mean and error factor. Examples of the methods used for several combinatorial cases are provided below.

C2.1 PARAMETER ESTIMATION USING DATA FROM DIFFERENT SOURCES

Using multiple reliability databases will typically cause a given active component to have various reliability estimates, each one from a different source. These various estimates can be viewed as independent samples from the same distribution, g , representing the source-to-source variability, also called population variability, of the component reliability (Ref. C5.4, Section 8.1). The objective of this section is to outline the methodology for developing the population-variability distribution of active components in the preclosure safety analysis. In a Bayesian approach to reliability estimation, the population-variability distribution of a component constitutes an informative prior distribution for its reliability. This distribution is to be updated, as operating experience becomes available, to produce a reliability distribution specific to the component operated under geologic repository operations area (GROA) conditions. For the time being however, the components anticipated for use at the GROA are yet to be procured and operated. As a consequence, the population-variability distributions developed in this section both aim at and are limited to encompassing the actual component reliability distributions that will be observed at the GROA when operating experience becomes available.

A parametric empirical Bayes method is used to develop the population-variability distributions of active components considered in the preclosure safety analysis. As indicated in “Bayesian Parameter Estimation in Probabilistic Risk Assessment.” (Ref. C5.44, Section 5.1.2), this method is a pragmatic approach that has been used in PRA-related applications; it involves specifying the functional form of the prior population-variability distribution, and fitting the prior to available data, using classical techniques, for example, the maximum likelihood method. A discussion of the adequacy of the parametric empirical Bayes method for determining the population-variability distribution is given at the end of this section.

Applying the parametric empirical Bayes method requires first to categorize the reliability data sources into two types: those that provide information on exposure data (i.e., the number of failures that were recorded over an exposure time (in case of a failure rate) or over a number of demands (in case of a failure probability), and those that do not provide such information). In the latter case, reliability estimates for a failure rate or failure probability are provided in the form of a mean or a median value, along with an uncertainty estimate, typically an error factor.

For each data source, the reliability information about a component's failure rate or failure probability is mathematically represented by its likelihood function. If exposure data are provided, the likelihood function takes the form of a Poisson distribution (for failure rates), or a binomial distribution (for failure probabilities) (Ref. C5.44, Section 4.2). When no exposure data are available, the reliability estimates for failure rates or failure probabilities are interpreted as expert opinion, for which an adequate representation of the likelihood function is a lognormal distribution ((Ref. C5.44, Section 4.4) and (Ref. C5.27, pp. 312, 314, and 315)).

The next step is to specify the form of the population-variability distribution. In its simplest form, the parametric empirical Bayes method only considers exposure data and employs distributions that are conjugate to the likelihood function (i.e., a gamma distribution if the likelihood is a Poisson distribution, and a beta distribution if the likelihood is binomial) (Ref. C5.4, Section 8.2.1), which have the advantage of resulting in relatively simpler calculations. This technique however is not applicable when both exposure data and expert opinion are to be taken into consideration, because no conjugate distribution exists in this situation. Following the approach of "The Combined Use of Data and Expert Estimates in Population Variability Analysis," (Ref. C5.27, Section 3.1), the population-variability distribution in this case is chosen to be lognormal. More generally, for consistency, the parametric empirical Bayes method is applied using the lognormal functional form for the population-variability distributions regardless of the type of reliability data available for the component considered (exposure data, expert opinion, or a combination of the two). In the rest of this section, the population-variability distribution in its lognormal form is noted $g(x, \nu, \tau)$, where x is the reliability parameter for the component (failure rate or failure probability), and ν and τ , the two unknowns to be determined, are respectively the mean and standard deviation of the normal distribution associated with the lognormal. The use of a lognormal distribution is appropriate for modeling the population-variability of failure rates and failure probabilities, provided in the latter case that any tail truncation above $x = 1$ has a negligible effect (Ref. C5.44, p. 99). The validity of this can be confirmed by selecting the failure probability with the highest mean and the most skewed lognormal distribution and calculating what the probability is of exceeding 1. In Table C4-1, PRV-FOD fits this profile, with a mean failure probability of 6.54E-03 and an error factor of 27.2. The probability that the distribution exceeds 1 is 2E-04. Stated equivalently, 99.98 percent of the values taken by the distribution are less than 1. This confirms that the use of a truncated lognormal distribution to represent the probability distribution is appropriate.

To determine ν and τ , it is first necessary to express the likelihood for each data source as a function of ν and τ only (i.e., unconditionally on x). This is done by integrating, over all possible values of x , the likelihood function evaluated at x , weighted by the probability of observing x , given ν and τ . For example, if the data source i indicates that r failures of a component occurred

out of n demands, the associated likelihood function $L_i(v, \tau)$, unconditional on the failure probability x , is as follows:

$$L_i(v, \tau) = \int_0^1 \text{Binom}(x, r, n) \times g(x, v, \tau) dx \quad (\text{Eq. C-2})$$

where $\text{Binom}(x, r, n)$ represents the binomial distribution evaluated for r failures out of n demands, given a failure probability equal to x , and $g(x, v, \tau)$ is defined as previously indicated. This equation is similar to that shown in “Bayesian Parameter Estimation in Probabilistic Risk Assessment.” (Ref. C5.44, Equation 37). If the component reliability was expressed in terms of a failure rate and the data source provided exposure data, the binomial distribution in Equation C-2 would be replaced by a Poisson distribution. If the data source provided expert opinion only (no exposure data), the binomial distribution in Equation C-2 would be replaced by a lognormal distribution.

The maximum likelihood method is an acceptable method to determine v and τ (Ref. C5.44, p. 101). The maximum likelihood estimators for v and τ are obtained by maximizing the likelihood function for the entire set of data sources. Given the fact that the data sources are independent, the likelihood function is the product of the individual likelihood functions for each data source (Ref. C5.27, Equation 4). To find the maximum likelihood estimators for v and τ , it is equivalent and computationally convenient to maximize the log-likelihood function, which is the sum of the logarithms of the likelihood function for each data source.

The calculation of v and τ completely determines the population-variability distribution g for the reliability of a given active component. The associated parameters to be plugged into SAPHIRE are the mean and the error factor of the lognormal distribution g , which are calculated using the formulas given in NUREG/CR-6823 (Ref. C5.4, Section A.7.3). Specifically, the mean of the lognormal distribution is equal to $\exp(v + \tau^2/2)$ and the error factor is equal to $\exp(1.645 \times \tau)$.

The selection of the parametric empirical Bayes method to determine the population-variability distribution is now discussed. This method provides a single “best” solution, while other techniques, such as the hierarchical Bayes method (Ref. C5.4, Section 8.3) differ by using a weighted mix of distributions of the chosen model, which incorporate epistemic (state of knowledge) uncertainty about the model. The parametric empirical Bayes method does not embed epistemic uncertainty but was nevertheless employed because of its satisfactory results for the majority of active components modeled in the preclosure safety analysis. The general adequacy of the method was confirmed by comparing its results to those obtained based on an example using a state-of-knowledge-informed approach (Ref. C5.27). The example involves twelve hypothetical data sources, each documenting the failure rate of motor-driven pumps either in terms of expert judgment or exposure data (Ref. C5.27, Table 1). Table C2.1-1 compares the percentiles predicted by the parametric empirical Bayes method and those found in “The Combined Use of Data and Expert Estimates in Population Variability Analysis.” (Ref. C5.27, Table 4). Overall, the percentiles appear to be similar, with a key metric of the distributions, their mean, being nearly identical, and the medians being comparable. Percentiles at the tails of the distributions show more differences, the parametric empirical Bayes method yielding a

population-variability distribution more spread out overall than the state-of-knowledge-informed distribution (Ref. C5.27).

Table C2.1-1. Comparison of Results of Parametric Empirical Bayes and Results Reported by Lopez Droguett et al.

Population-Variability Value	Parametric Empirical Bayes Method ^a	Lopez Droguett Results ^b
Mean	6.00×10^{-5}	6.05×10^{-5}
1 st percentile	1.32×10^{-7}	3.16×10^{-7}
5 th percentile	4.75×10^{-7}	1.38×10^{-6}
10 th percentile	9.38×10^{-7}	2.67×10^{-6}
50 th percentile (median)	1.04×10^{-5}	1.61×10^{-5}
90 th percentile	1.14×10^{-4}	7.79×10^{-5}
95 th percentile	2.26×10^{-4}	1.36×10^{-4}
99 th percentile	8.10×10^{-4}	4.85×10^{-4}

NOTE: ^a Derivation of the results is given in the following section, Example of Development of Population-Variability Distribution.

^b ("The Combined Use of Data and Expert Estimates in Population Variability Analysis." Reliability Engineering and System Safety, 83 (Ref. C5.27, Table 1)

Source: Ref. C5.27, Table 1

An adjustment to the parametric empirical Bayes method was done in a few instances where the error factor of the calculated lognormal distribution was found to be excessive. In a synthetic examination of the failure rates of various components, "External Maintenance Rate Prediction and Design Concepts for High Reliability and Availability on Space Station Freedom," *Reliability Engineering and System Safety*, 47 (Ref. C5.19, Figure 3) finds that electromechanical and mechanical components have, overall, a range of variation approximately between 2×10^{-8} /hr (5th percentile) and 6×10^{-5} /hr (95th percentile). Using the definition of the error factor given in NUREG/CR-6823, (Ref. C5.4, Section A.7.3), this corresponds to an error factor of $\sqrt{6 \cdot 10^{-5} / 2 \cdot 10^{-8}} = 55$. Therefore, in the preclosure safety analysis, it is considered that lognormal distributions resulting from the empirical Bayes method that yield error factors with a value greater than 55 are too diffuse to adequately represent the population-variability distribution of a component. In such instances (two such cases in the entire PCSA database, when the error factors from the Bayesian estimation were greater than 200), the lognormal distribution used to represent the population-variability is modified as follows. It has the same median as that predicted by the parametric empirical Bayes method, and its error factor is assigned a value of 55. The median is selected as the unvarying parameter because, contrary to the mean, it is not sensitive to the behavior of the tails of the distribution and therefore is unaffected by the value taken by the error factor. Based on NUREG/CR-6823, (Ref. C5.4, Section A.7.3), the median is calculated as $\exp(v)$, where v is obtained by the maximum likelihood estimation.

A limitation of the parametric empirical Bayes method that prevented its use for all active components of the preclosure safety analysis is that the calculated lognormal distribution can

sometimes have a very small error factor (with a value around 1), corresponding to a distribution overly narrow to represent a population-variability distribution. As indicated in NUREG/CR-6823, (Ref. C5.4, p. 8-4), this situation can arise when the reliability data sources provide similar estimates for a component reliability. The inadequacy of the parametric empirical Bayes method in such situations is made apparent by plotting the probability density function of the lognormal distribution and comparing it with the likelihood functions associated with the reliability estimates of each data source. In the cases where the lognormal distribution does not approximately encompass the likelihood functions yielded by the data sources, it is not used to model the population-variability distribution. Instead, this distribution is modeled using a data source that yields a more diffuse likelihood. In the other cases, the lognormal distribution approximately encompasses the likelihood functions yielded by the data sources, showing that the parametric empirical Bayes method is adequate. An illustration of a graph plotting the population-variability distribution along with the likelihood functions from data, based on the example of the Lopez Droguett et al. paper (Ref. C5.27) is provided below.

Example of Development of Population-Variability Distribution

Mathcad is used to calculate the population-variability distribution of active components. An illustration of such a calculation is given using the example in “The Combined Use of Data and Expert Estimates in Population Variability Analysis.” (Ref. C5.27, Table 1). In this example, several data sources supply information about the reliability of motor-driven pumps, as follows:

Four data sources supply point estimates of the failure rates, along with a range (error) factor. This information is given in the following matrix, where the first column contains the estimated hourly failure rate (considered to be a median value) and the second column the associated error factor:

$$A := \begin{pmatrix} 3.0 \cdot 10^{-5} & 5 \\ 2.1 \cdot 10^{-5} & 3 \\ 2.0 \cdot 10^{-5} & 10 \\ 2.53 \cdot 10^{-5} & 10 \end{pmatrix}$$

In addition, eight data sources supply exposure data, which are given in the following matrix, where a recorded number of failures is shown in the first column, and the associated operating time (in hours) is shown in the second.

$$B := \begin{pmatrix} 0 & 76000 \\ 0 & 152000 \\ 0 & 74000 \\ 2 & 74000 \\ 0 & 48000 \\ 3 & 76000 \\ 9 & 10200 \\ 2 & 48000 \end{pmatrix}$$

The population-variability distribution g of the failure rate x is approximated by a lognormal distribution whose unknown parameters, ν and τ , respectively the mean and standard deviation of the associated normal distribution, are to be determined. Calculating ν and τ involves calculating the likelihood function associated with the reliability information in each data source. This is done as follows:

For a data source providing a failure rate point estimate, the likelihood function is a lognormal distribution, function of the failure rate x , and characterized by its median value and associated error factor shown in the matrix A . In Mathcad, the parameters required for defining a lognormal distribution are the mean and standard deviation of the associated normal distribution. Based on the formulas given in NUREG/CR-6823 (Ref. C5.4, Section A.7.3), the mean of the associated normal distribution is the natural logarithm of the median failure rate, and the standard deviation of the associated normal distribution is $\ln(EF)/1.645$, where EF is the error factor.

Because the unknowns to be determined are ν and τ , the likelihood function is expressed as a function unconditional on the value of x . This is done by integrating the likelihood function over all possible values of x (i.e., theoretically, from 0 to infinity) and weighting by the probability of having a value of x , conditional on observing ν and τ . In practice, to facilitate the numerical integration on Mathcad, the integration is performed on a range that encompasses credible values for x . In this example, the failure rate range considered varies from $10^{-8}/\text{hr}$ to $10^{-2}/\text{hr}$. Thus, the likelihood functions, unconditional on x , for each of the data source in the matrix A , are calculated as follows:

$$a := 1..4 \quad fe(a, x) := dlnorm\left(x, \ln(A_{a,1}), \frac{\ln(A_{a,2})}{1.645}\right) \quad (\text{Eq. C-3})$$

$$LA(a, \nu, \tau) := \int_{10^{-8}}^{10^{-2}} fe(a, x) \cdot dlnorm(x, \nu, \tau) dx \quad (\text{Eq. C-4})$$

(In the above formulas, a is an index used to particularize a likelihood function to a data source in the matrix A .)

For a data source providing exposure data (given in the form of a number n of recorded failures over an exposure time t), the likelihood function is a Poisson distribution, expressing the

probability that n failures are observed when the expected number of failures is x times t . Here also, the likelihood needs to be expressed as a function unconditional on the failure rate x , which is done by integrating x out, in a similar manner as above:

$$b := 1..8 \qquad fd(b, x) := dpois(B_{b,1}, B_{b,2} \cdot x) \qquad \text{(Eq. C-5)}$$

$$LB(b, \nu, \tau) := \int_{10^{-8}}^{10^{-2}} fd(b, x) \cdot dlnorm(x, \nu, \tau) dx \qquad \text{(Eq. C-6)}$$

(In the above formulas, b is an index used to particularize a likelihood function to a data source in the matrix B .)

The maximum likelihood method is used to calculate ν and τ . This involves maximizing the likelihood function for the entire set of data sources. This likelihood function is the product of the individual likelihood function for each data source (this is because the data sources are independent from each other). It is equivalent and computationally convenient to find the maximum likelihood estimators for ν and τ by using the sum of the log-likelihood (logarithm of the likelihood) of each data source.

Therefore, the log-likelihood function to be maximized is:

$$L(\nu, \tau) := \sum_{a=1}^4 \ln(LA(a, \nu, \tau)) + \sum_{b=1}^8 \ln(LB(b, \nu, \tau)) \qquad \text{(Eq. C-7)}$$

To maximize a function, Mathcad requires guess values and a range over which to search for maxima. The quantity ν represents the logarithm of a failure rate, which is expected to be in the 10^{-6} /hr range. Therefore, a guess value for ν is:

$$\nu := \ln(10^{-6}) \qquad \nu = -13.8$$

Based on a typical error factor value of 10, a guess value for τ is:

$$\tau := \frac{\ln(10)}{1.645} \qquad \tau = 1.4$$

A reasonable range over which to perform the likelihood maximization is as follows:

<i>Given</i>	$\nu > -20$	$\nu < -1$
	$\tau > 0.01$	$\tau < 5$

The maximum likelihood estimators for ν and τ are:

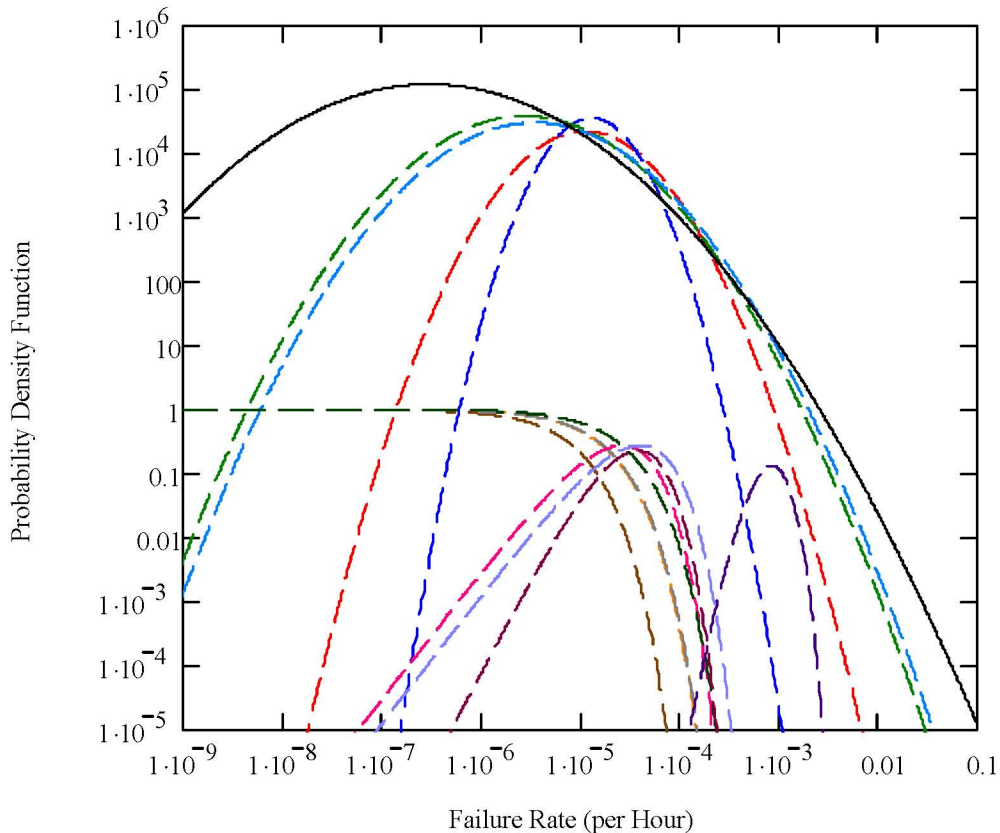
$$\begin{aligned} \underline{L}_1 &:= \text{Maximize}(L, \nu, \tau) & \underline{\nu} &:= L1 \quad \nu = -11.478 \\ \underline{\tau} &:= L2 & \tau &= 1.874 \end{aligned}$$

Therefore, the mean and error factors of the population-variability distribution for the failure rate are (based on the formula in NUREG/CR-6823 (Ref. C5.4, Section A.7.3)):

$$\begin{aligned} \underline{m} &:= \exp\left(\nu + \frac{2}{\tau}\right) & m &= 6.00 \times 10^{-5} \quad \text{per hour} \\ EF &:= \exp(1.645 \cdot \tau) & EF &= 21.8 \end{aligned}$$

Notable percentiles of the population-variability distribution are as follows (expressed as hourly failure rates) and shown in Figure C2.1-1:

1 st percentile:	$qlnorm(0.01, \nu, \tau) = 1.32 \times 10^{-7}$
5 th percentile:	$qlnorm(0.05, \nu, \tau) = 4.75 \times 10^{-7}$
10 th percentile:	$qlnorm(0.10, \nu, \tau) = 9.38 \times 10^{-7}$
50 th percentile:	$qlnorm(0.50, \nu, \tau) = 1.04 \times 10^{-5}$
90 th percentile:	$qlnorm(0.90, \nu, \tau) = 1.14 \times 10^{-4}$
95 th percentile:	$qlnorm(0.95, \nu, \tau) = 2.26 \times 10^{-4}$
99 th percentile:	$qlnorm(0.99, \nu, \tau) = 8.10 \times 10^{-4}$



Source: Original

Figure C2.1-1. Likelihood Functions from Data Sources (Dashed Lines) and Population-Variability Probability Density Function (Solid Line)

C2.2 PARAMETER ESTIMATION IN CASE ONLY ONE DATA SOURCE IS AVAILABLE

To be developed, a population-variability distribution requires at least two data sources, and therefore the previous method is not applicable when only one data source is available. In this case, the probability distribution for the reliability parameter of an active component is that yielded by the data source. For example, if the data source provides a mean and an error factor for the component reliability parameter, the probability distribution is modeled in SAPHIRE as a lognormal distribution with that mean and that error factor. If the data source does not readily provide a probability distribution, but instead exposure data (i.e., a number of recorded failures over an exposure time for failure rates, or over a number of demands for failure probabilities) the probability distribution for the reliability parameter is developed through a Bayesian update using Jeffreys' noninformative prior distribution. As indicated in NUREG/CR-6823 (Ref. C5.4, Section 6.2.2.5.2), this noninformative prior conveys little prior belief or information, thus allowing the data to speak for themselves.

As mentioned in "Bayesian Parameter Estimation in Probabilistic Risk Assessment," (Ref. C5.44, Section 4.2), the likelihood function associated with exposure data is either a Poisson distribution (in the case of failure rates), or a binomial distribution (in the case of failure probabilities).

Applying Bayes' theorem with Jeffreys' noninformative prior in conjunction with a Poisson likelihood function characterized by r recorded failures over an exposure time t results in a closed-form posterior distribution, namely a gamma distribution, characterized by a shape parameter equal to $0.5 + r$, and a scale parameter equal to t ; the mean of this distribution is $(0.5 + r)/t$ (Ref. C5.4, Sections 6.2.2.5.2 and A7.6). In SAPHIRE, this distribution is characterized by its mean and by its shape parameter (i.e., $0.5 + r$).

Applying Bayes' theorem with Jeffreys' noninformative prior in conjunction with a binomial likelihood function characterized by r recorded failures out of n demands results in a closed-form posterior distribution, namely a beta distribution, characterized by a parameter " a " equal to $0.5 + r$, and a parameter " b " equal to $n - r + 0.5$; the mean of this distribution is $(0.5 + r)/(n + 1)$ (Ref. C5.4, Sections 6.3.2.3.2 and A7.8). In SAPHIRE, this distribution is characterized by its mean and by the parameter " b " (i.e., $n - r + 0.5$).

C3 COMMON-CAUSE FAILURE DATA

Dependent failures are modeled in event tree and fault tree logic models, with potential dependent failures modeled explicitly via the logic models, whenever possible. For example, failure of the HVAC system is explicitly dependent upon failures in the electrical supply systems that are modeled in the fault trees. Similarly, the effects of erroneous calibration or other human failure events can be explicitly included in the system fault tree models and the basic event probabilities considered during the human reliability analysis. Otherwise, potential dependencies known as CCFs are included in fault tree logic, but their probabilities are quantified by an implicit, parametric method. Therefore, another subtask of the active component reliability data analysis is to estimate common-cause failure probabilities.

Surveys of failure events in the nuclear industry have led to several parameter models. Of these, three are most commonly used: the Beta Factor method (Ref. C5.18), the Multiple Greek Letter method (Ref. C5.29) and (Ref. C5.30), and the Alpha Factor method (Ref. C5.31). These methods do not require an explicit knowledge of the dependence failure mode. For the YMP PCSA, CCF rates or probabilities were estimated using the alpha factor method described in NUREG/CR-5485 (Ref. C5.31).

The vast majority of the equipment types for which CCF basic events were modeled in the YMP PCSA are not covered by the detailed component-specific alpha factor sources based on commercial nuclear plant equipment. Therefore, it was necessary to use alpha factors to address the common-cause failure estimates for crane hoist wire ropes, gear boxes, over-torque sensors and the like.

The alpha factor method provides a model to treat CCF probabilities of k -of- m components. In addition, industry-wide alpha factors have been developed for the U.S. Nuclear Regulatory Commission from experience data collected at nuclear power plants. The data analysis reported in NUREG/CR-5485 (Ref. C5.31) consisted of:

1. Identifying the number of redundant components in each subsystem being reported (e.g., two, three, or four (this is termed the common-cause component group (CCCG) of size m)).

2. Partitioning the total number of reported failure events for a given component into the number of components that failed together, i.e., $k = 1$ for one component at a time, $k = 2$ for two components at a time, $k = 3$ for three components at a time, up to m for failure of all components in a given CCF group.
3. Estimating the alpha factor for a given component type based on its definition as the fraction of total failure events that involve k component failures due to a common cause, for a system of m redundant components, using the alpha factor estimator from NUREG/CR-5485 (Ref, C5.31, Table 5-10), as shown below:

$$\alpha_k^m = \frac{n_k}{\sum_{j=1}^m n_j} \quad k = 1, \dots, m ;$$

where n_i is the number of basic events observed that involve failure of i similar components.

4. Performing statistical analysis and curve fitting to define the mean and uncertainty range for alpha factors for various CCF group sizes up to eight.

The data analysis also produced industry-wide prior distributions for the alpha factors for each CCF size, based on all CCF events in their database. Events were mapped to a given CCF size, the maximum likelihood estimator obtained and fit to a constrained noninformative prior distribution. The parameter A_T of a Dirichlet distribution was then calculated for each alpha and the results combined using the geometric mean. The results are the industry-wide mean alpha factors and beta uncertainty distributions reported in of NUREG/CR-5485 (Ref. C5.31, Table 5-11) shown in Table C3-1:

Table C3-1. Industry-Wide Alpha Factors

Table 5-11. Generic prior distributions for various system sizes.

CCCG Size m	α -Factor	Distributions Parameters		Percentiles			Mean
		a	b	P ₀₅	P ₅₀	P ₉₅	
2	α_1	9.5300	0.470	8.20E-01	9.78E-01	1.00E-00	0.95300
	α_2	0.4700	9.530	1.42E-04	2.16E-02	1.81E-01	0.04700
3	α_1	15.2000	0.800	8.42E-01	9.67E-01	9.99E-01	0.95000
	α_2	0.3872	15.613	2.10E-05	8.79E-03	1.01E-01	0.02420
	α_3	0.4128	15.587	3.45E-05	1.01E-02	1.05E-01	0.02580
4	α_1	24.7000	1.300	8.67E-01	9.61E-01	9.95E-01	0.95000
	α_2	0.5538	25.446	1.44E-04	1.08E-02	7.81E-02	0.02130
	α_3	0.2626	25.737	2.98E-07	1.99E-03	4.82E-02	0.01010
	α_4	0.4836	25.516	6.29E-05	8.42E-03	7.17E-02	0.01860
5	α_1	38.042	1.958	8.86E-01	9.58E-01	9.91E-01	0.95106
	α_2	0.7280	39.272	3.72E-04	1.10E-02	6.05E-02	0.01820
	α_3	0.4120	39.588	1.32E-05	3.93E-03	4.22E-02	0.01030
	α_4	0.2336	39.766	4.57E-08	8.97E-04	2.89E-02	0.00584
	α_5	0.5840	39.416	1.24E-04	7.66E-03	5.27E-02	0.01460
6	α_1	50.4724	2.528	8.97E-01	9.58E-01	9.89E-01	0.95231
	α_2	0.7791	52.221	3.76E-04	9.20E-03	4.78E-02	0.01470
	α_3	0.5406	52.459	6.04E-05	5.02E-03	3.79E-02	0.01020
	α_4	0.3127	52.687	9.28E-07	1.56E-03	2.66E-02	0.00590
	α_5	0.2433	52.757	5.77E-08	7.67E-04	2.24E-02	0.00459
	α_6	0.6519	52.348	1.66E-04	6.93E-03	4.27E-02	0.01230
7	α_1	74.5360	3.464	9.12E-01	9.59E-01	9.86E-01	0.95559
	α_2	0.9906	77.009	6.44E-04	8.84E-03	3.79E-02	0.01270
	α_3	0.6817	77.318	1.39E-04	5.05E-03	2.99E-02	0.00874
	α_4	0.4891	77.511	2.21E-05	2.82E-03	2.42E-02	0.00627
	α_5	0.2941	77.706	3.39E-07	8.97E-04	1.74E-02	0.00377
	α_6	0.2051	77.795	3.84E-09	2.94E-04	1.35E-02	0.00263
	α_7	0.8034	77.197	2.89E-04	6.52E-03	3.32E-02	0.01030
8	α_1	97.6507	4.349	9.20E-01	9.60E-01	9.84E-01	0.95736
	α_2	1.1118	100.888	7.25E-04	7.91E-03	3.13E-02	0.01090
	α_3	0.7915	101.209	2.07E-04	4.87E-03	2.52E-02	0.00776
	α_4	0.6253	101.375	6.92E-05	3.34E-03	2.17E-02	0.00613
	α_5	0.4417	101.558	8.51E-06	1.76E-03	1.74E-02	0.00433
	α_6	0.2581	101.742	6.09E-08	4.74E-04	1.21E-02	0.00253
	α_7	0.1969	101.803	1.59E-09	1.93E-04	1.00E-02	0.00193
	α_8	0.9241	101.076	3.82E-04	6.12E-03	2.78E-02	0.00906

Source: NUREG/CR-5485 (Ref. C5.31)

Values from Table C3-1 are applied to the YMP PCSA using the CCF algorithms contained in the SAPHIRE code compound event library to combine the random failure probabilities of the events in the CCF group with the appropriate alpha factors for *k*-of-*m* components for failure-on-demand events (e.g., pump failure to start). For example, for a 2-out-of-2 failure-on-demand event, the mean alpha factors of 0.953 and 0.047 shown in the far right column of Table C3-1 associated with α_1 and α_2 are input into a compound event with the two component demand failures and the 2 of 2 failure criteria. The CCF algorithm for the alpha-factor common-cause

model with staggered testing is selected from the SAPHIRE code library of potential common-cause models to yield the common-cause failure probability..

For failure-to-operate events (e.g., pump fails to run), the mean alpha factor (M) for events with more than one failure from Table C3-1 is divided by 2 in accordance with NUREG/CR-5485 (Ref. C5.31). (The mean alpha factor for events with one failure is computed as 1 minus the sum of the remaining alpha factors.) In addition, the parameter b associated with the beta distribution function for the alpha factor is modified to reflect the change in the alpha factor mean value while preserving the coefficient of variation from the distribution described by the parameters presented in Table C3-1. To preserve the coefficient of variation, the variance (V) of each failure-to-operate alpha factor is set to one fourth that of the corresponding failure-on-demand alpha factor. The factor of 4 results from reducing the standard deviation by a factor of 2, like the mean. Because the variance is the square of the standard deviation, the variance decreases by a factor of 4. The following formulas give the mean and variance of a beta distribution in terms of the parameters a and b (Ref. C5.4, Section A.7.8). To derive an alpha factor for a failure-to-operate event, the mean alpha factor is taken from Table C3-1 (or computed from the following formula) and divided by 2.

$$M = \frac{a}{a+b}.$$

Then, the variance is calculated from the following formula and divided by 4.

$$V = \frac{a \cdot b}{(a+b)^2 \cdot (a+b+1)}$$

Inserting the modified values of M and V into the following formula (which can be derived from the two formulas above) yields the parameter b .

$$b = \frac{(M - M^2 - V) \cdot (1 - M)}{V}.$$

Table C3-2 provides values taken or derived from Table C3-1 in the form required by SAPHIRE, that is, the mean alpha factor and the parameter b , which together completely specify the uncertainty distribution.

Table C3-2. Alpha Factor Inputs for SAPHIRE

SAPHIRE Template Event Identifier ^a	Mean Alpha Factor	Uncertainty Parameter (b)
ALPHADEM-1OF2	0.95300	0.470
ALPHADEM-2OF2	0.04700	9.530
ALPHARUN-1OF2	0.97650	0.0506
ALPHARUN-2OF2	0.02350	21.036
ALPHADEM-1OF3	0.95000	0.800
ALPHADEM-2OF3	0.02420	15.613
ALPHADEM-3OF3	0.02580	15.587
ALPHARUN-1OF3	0.97500	0.847
ALPHARUN-2OF3	0.01210	33.018
ALPHARUN-3OF3	0.01290	33.018
ALPHADEM-1OF4	0.95000	1.300
ALPHADEM-2OF4	0.02130	25.446
ALPHADEM-3OF4	0.01010	25.737
ALPHADEM-4OF4	0.01860	25.516
ALPHARUN-1OF4	0.97500	1.361
ALPHARUN-2OF4	0.01065	53.016
ALPHARUN-3OF4	0.00505	53.005
ALPHARUN-4OF4	0.00930	53.012

NOTE: ^a The identifier follows the pattern ALPHAXXX-*k*OF*m*, where XXX = DEM for failures on demand, XXX = RUN for failures during operation, *m* represents the size of the CCF group, and *k* is the number of failed items within the CCF group.

This approach was considered to provide conservative CCF data for all the component types for which common-cause failures were modeled. This was considered particularly important since the YMP has never operated and therefore the applicability of conventional nuclear plant alpha factors could not be justified.

The conservatism of this approach can be demonstrated by comparing the alpha factors used for the PCSA diesel generator CCF events to those posted on the U.S. Nuclear Regulatory Commission website for use in Probabilistic Risk Assessment studies of commercial nuclear power plants in the U.S.

The alpha factor used for the PCSA for 2 of 2 diesel generators failing to start was the 0.047 value cited earlier, while the mean alpha factor for a CCG=2 cited by the NRC (Ref. C5.36) is 0.0136.

Diesel generators are the only component types for which such a comparison can be made since the other YMP component types for which CCFs were modeled were not covered by the NRC equipment-specific alpha factors.

C4 ACTIVE COMPONENT RELIABILITY ESTIMATES INPUT TO SAPHIRE

Since the primary active component reliability data task objective is to support the quantification of fault tree models developed in SAPHIRE by the system analysts, the output data had to conform to the format appropriate for input to the SAPHIRE code.

SAPHIRE provides template data to the fault tree models in the form of three input comma delimited files:

- BEA – attributes to assign information to the proper SAPHIRE fields
- BED – descriptions of the component type name and failure mode
- BEI – information on the failure rate or probability estimates and distributions used.

Demonstration files for the .BEA, .BED and .BEI template data files provided with SAPHIRE were originally used to construct the PCSA template data files to ensure the proper formatting of the data for use by the fault tree models. In general, the .BEA file provides attribute designators for the code to implement such that the template data is properly assigned to the appropriate fields in SAPHIRE. The .BED file allows description information to be entered and linked to the template data name or designator (which in the YMP PCSA case was the TYP-FM coding). Examples of descriptions used for the PCSA template data were Clutch Failed to Operate, Relay Spurious Operation, Position Sensor Fails on Demand, and Wire Rope Breaks. The .BEI file contains the actual active component reliability parameters, namely the mean value and uncertainty parameter, either the Lognormal Error Factor, or the shape parameter of the beta or gamma distributions.

Geometric means of the input parameters from the industry-wide data sources were initially used as screening values for each TYP-FM and were entered into the .BEI file, along with a default Error Factor of 10. Once the Bayesian combination process was completed for all 275 TYP-FM combinations, mean and uncertainty parameter information was entered into the BEA files, and tested in SAPHIRE before being distributed to the systems analysts.

Failure probability per demand information was entered as SAPHIRE Calculation Type 1 for a simple probability and failure rate per hour information was entered as SAPHIRE Calculation Type 3 as a mean failure rate in the lambda field. Calc Type 3 uses the formula $P = 1 - \exp(-\lambda T_m)$, where λ is the mean failure rate (or lambda) and T_m is the mission time. Mission time is defined in the SAPHIRE Basics manual as "...the period of time that a component is required to operate in order to characterize the component operation as successful." Since the template data was to be used for all YMP facilities while the mission times would be system-specific, the mission time field in the three template data files was left blank and these times were instead input individually by the systems analysts.

The correlation class field was also used for the YMP template data files "to account for data dependencies among like events in the database" during the uncertainty analysis, as stated in the SAPHIRE Basics manual. This meant that all components in the same correlation class would be treated the same during the uncertainty analysis. This feature of SAPHIRE is based upon the observations documented (Ref. C5.2) that in the risk models, all components of the same type are quantified with the same failure rate or probability, therefore it is appropriate to group together

the experience of all the nominally identified components in the same facility. Therefore, all components of the same type and failure mode are aggregated into a single number, meaning that the dependency between components of the same class must somehow be addressed. For example, if multiple motor-operated valves needed to open for success and all are assigned the same failure probability, then these basic events needed to be correlated via being assigned the same correlation class in the .BEI file. However, if different probabilities were to be used for different motor-operated valves based on the data, then the basic events would not be correlated. In all cases, a correlation class identifier, using the TYP-FM acronyms, was input to the .BEI file to indicate that all equipment with in the same TYP-FM should be correlated by the SAPHIRE model. SAPHIRE then would sample from one distribution and then use this sampled probability for all other basic events with the same correlation class.

The template data was also identified by TYP-FM combination and was utilized by the fault tree models by being imported into SAPHIRE using the MAR-D portion of the code, then by using the Modify Event feature to link the template data to each basic event in the fault tree. This permitted each active component of the same type and failure mode to utilize the same failure estimate and uncertainty information, based on the results of the industry-wide data investigation and Bayesian combination process.

Table C4-1 shows the active component reliability estimates that were input to SAPHIRE as template data for fault tree model quantification.

Table C4-1. Active Component Reliability Estimates Entered into SAPHIRE Models

TYP-FM	Component Name & Failure Mode	Dist Type	Uncertainty Value	Demand Probability	Hourly Failure Rate	Number of Inputs	Input Data Sources ^a
AHU-FTR	Air Handling Unit Failure to Run	G	5.00E-01	—	3.80E-06	1 source; N/D	NUREG/CR-6928 (Ref. C5. 16)
ALM-SPO	Alarm/Annunciator Spurious Operation	L	1.30E+01	—	4.74E-07	5 sources N/D; 1 source mean	IEEE-500 (Ref. C5.23), NPRD-95 (Ref. C5.40)
AT-FOH	Actuator (Electrical) Failure	L	1.24E+01	—	7.54E-05	3 sources; N/D	NPRD-95 (Ref. C5.40)
ATH-FOH	Actuator (Hydraulic) Failure	L	3.81E+01	—	8.91E-04	4 sources; N/D	NPRD-95 (Ref. C5.40)
ATP-SPO	Actuator (Pneumatic Piston) Spurious Operation	L	5.00E+00	—	1.34E-06	1 source; mean + EF	NPRD-95 (Ref. C5.40)
AXL-FOH	Axle Failure	G	5.00E-01	—	1.60E-08	1 source; N/D	NPRD-95 (Ref. C5.40)
B38-FOH	Bearing Failure	L	1.13E+01	—	2.50E-06	8 sources; N/D	NPRD-95 (Ref. C5.40)
BEA-BRK	Lifting Beam/Boom Breaks	G	1.50E+00	—	2.40E-08	1 source; N/D	NPRD-95 (Ref. C5.40)
BLD-RUP	Air Bag Ruptures	B	1.10E+04	1.36E-04	—	1 source; N/D	BSC 2007 (Ref. C5.7)
BLK-FOD	Block or Sheaves Failure on Demand	B	1.30E+06	1.15E-06	—	1 source; N/D	NPRD-95 (Ref. C5.40)
BRH-FOD	Brake (Hydraulic) Failure on Demand	L	5.50E+01	8.96E-06	—	3 sources N/D; 1 source mean + EF	NPRD-95 (Ref. C5.40)
BRK-FOD	Brake Failure on Demand	L	6.30E+00	1.46E-06	—	3 sources; mean + EF	EPRI PRA (Ref. C5.8)
BRK-FOH	Brake (Electric) Failure	G	2.50E+00	—	4.40E-06	1 source; N/D	NPRD-95 (Ref. C5.40)
BRP-FOD	Brake (Pneumatic) Failure on Demand	L	2.55E+00	5.02E-05	—	4 sources; N/D	NPRD-95 (Ref. C5.40)
BRP-FOH	Brake (Pneumatic) Failure	L	2.55E+00	—	8.38E-06	4 sources; N/D	NPRD-95 (Ref. C5.40)
BTR-FOD	Battery No Output Given Challenge	B	6.05E+01	8.20E-03	—	1 source; N/D	NUREG/CR-4639 (Ref. C5.39)
BTR-FOH	Battery Failure	L	4.30E+00	—	4.29E-06	12 sources N/D; 8 sources mean + EF	CCPS (Ref. C5.1), N-Reactor (Ref. C5.46), NPRD-95 (Ref. C5.40), NUREG/CR-4639 (Ref. C5.39), NUREG/CR-6928 (Ref. C5. 16), SAIC Umatilla (Ref. C5.41)
BUA-FOH	AC Bus Failure	L	3.08E+00	—	6.10E-07	3 sources; N/D	IEEE 493 (Ref. C5. 22), NUREG/CR-6928 (Ref. C5. 16)

Table C4-1. Active Component Reliability Estimates Entered into SAPHIRE Models (Continued)

TYP-FM	Component Name & Failure Mode	Dist Type	Uncertainty Value	Demand Probability	Hourly Failure Rate	Number of Inputs	Input Data Sources ^a
BUD-FOH	DC Bus Failure	L	8.70E+01	—	2.40E-07	1 source mean + EF	IEEE-500 (Ref. C5.23)
BYC-FOH	Battery Charger Failure	L	1.00E+01	—	7.60E-06	1 source mean + EF	CCPS (Ref. C5.1)
C52-FOD	Circuit Breaker (AC) Fails on Demand	L	9.80E+00	2.24E-03	—	19 sources N/D; 1 source mean + EF	CCPS (Ref. C5.1), NUREG/CR-4639 (Ref. C5.39), SAIC Umatilla (Ref. C5.41), SRS Reactors (Ref. C5.5)
C52-SPO	Circuit Breaker (AC) Spurious Operation	L	2.29E+01	—	5.31E-06	12 sources N/D; 1 source mean + EF	CCPS (Ref. C5.1), MIL-HDBK-217F (Ref. C5.12), NUREG/CR-6928 (Ref. C5.16), NUREG/CR-4639 (Ref. C5.39), SAIC Umatilla (Ref. C5.41)
C72-SPO	Circuit Breaker (DC) Spurious Operation	L	1.20E+00	—	1.07E-06	3 sources N/D; 1 source mean + EF	CCPS (Ref. C5.1), MIL-HDBK-217F (Ref. C5.12), NUREG/CR-4639 (Ref. C5.39), NUREG/CR-6928 (Ref. C5.16)
CAM-FOH	Cam Lock Fails	L	8.30E+01	—	3.19E-06	4 sources N/D; 1 source mean + EF	NPRD-95 (Ref. C5.40)
CBP-OPC	Cables (Electrical Power) Open Circuit	G	5.00E-01	—	9.13E-08	1 source; N/D	NPRD-95 (Ref. C5.40)
CBP-SHC	Cables (Electrical Power) Short Circuit	G	5.00E-01	—	1.88E-08	1 source; N/D	NPRD-95 (Ref. C5.40)
CKV-FOD	Check Valve Fails on Demand	L	1.36E+01	6.62E-04	—	4 sources N/D; 7 sources mean + EF	CCPS (Ref. C5.1), N-Reactor (Ref. C5.46), NUREG/CR-4639 (Ref. C5.39), NUREG/CR-6928 (Ref. C5.16), SRS Reactors (Ref. C5.5)
CKV-FTX	Check Valve Fails to Check	L	1.50E+01	2.20E-03	—	1 source; mean + EF	CCPS (Ref. C5.1)
CON-FOH	Electrical Connector (Site Transporter) Failure	G	5.00E-01	—	7.14E-05	1 source; N/D	NPRD-95 (Ref. C5.40)
CPL-FOH	Coupling (Automatic) Failure	L	5.00E+00	—	1.91E-06	1 source mean + EF	AIAA (Ref. C5.11)
CPO-FOH	Control System Onboard (TEV or Trolley) Failure	G	9.85E+01	—	2.10E-08	1 source; N/D	NPRD-95 (Ref. C5.40)

Table C4-1. Active Component Reliability Estimates Entered into SAPHIRE Models (Continued)

TYP-FM	Component Name & Failure Mode	Dist Type	Uncertainty Value	Demand Probability	Hourly Failure Rate	Number of Inputs	Input Data Sources ^a
CRD-FOH	Card Reader Failure	L	5.00E+00	—	4.55E-05	1 source mean + EF	HID (Ref. C5.21)
CRN-DRP	200 Ton Crane Drop	L	4.32E+01	3.16E-05	—	2 sources N/D; 4 sources mean + EF	NUREG-0612 (Ref. C5.35), NUREG-1774 (Ref. C5.26), EPRI PRA (Ref. C5.8)
CRN-TBK	200 Ton Crane Two Block Drop	L	1.15E+01	4.41E-07	—	1 source N/D; 3 sources mean + EF	NUREG-0612 (Ref. C5.35), NUREG-1774 (Ref. C5.26)
CRS-DRP	200 Ton Crane Sling Drop	B	2.13E+04	1.17E-04	—	1 source; N/D	NUREG-1774 (Ref. C5.26)
CRW-DRP	WP (Non-Single Failure Proof) Crane Drop	B	3.27E+04	1.07E-04	—	1 source; N/D	NUREG-1774 (Ref. C5.26)
CRW-TBK	WP (Non-Single Failure Proof) Crane Two Block Drop	B	3.27E+04	4.59E-05	—	1 source; N/D	NUREG-1774 (Ref. C5.26)
CSC-FOH	Cask Cradle Failure	G	1.50E+00	—	4.81E-08	1 source; N/D	NPRD-95 (Ref. C5.40)
CT-FOD	Controller Mechanical Jamming	L	5.00E+00 ^b	4.00E-06	—	1 source; mean + EF	EPRI PRA (Ref. C5.8)
CT-FOH	Controller Failure	L	1.00E+01	—	6.88E-05	1 source mean + EF	CCPS (Ref. C5.1)
CT-SPO	Controller Spurious Operation	L	1.00E+01	—	2.27E-05	1 source mean + EF	CCPS (Ref. C5.1)
CTL-FOD	Logic Controller Fails on Demand	L	1.10E+01	2.03E-03	—	3 sources; N/D	NUREG/CR-6928 (Ref. C5.16)
DER-FOM	Derailment Failure per Mile	G	3.97E+03	—	1.18E-05	1 source; N/D	Federal Railroad Administration (Ref. C5.17)
DG-FTR	Diesel Generator Fails to Run	L	1.51E+01	—	4.08E-03	8 sources N/D; 1 source mean + EF	CCPS (Ref. C5.1), IEEE 493 (Ref. C5.22), NUREG/CR-4639 (Ref. C5.39), NUREG/CR-3831 (Ref. C5.24), NUREG/CR-6890 (Ref. C5.15), NUREG/CR-6928 (Ref. C5.16), SAIC Umatilla (Ref. C5.41), SRS Reactors (Ref. C5.5)

Table C4-1. Active Component Reliability Estimates Entered into SAPHIRE Models (Continued)

TYP-FM	Component Name & Failure Mode	Dist Type	Uncertainty Value	Demand Probability	Hourly Failure Rate	Number of Inputs	Input Data Sources ^a
DG-FTS	Diesel Generator Fails to Start	L	3.50E+00	8.38E-03	—	9 sources N/D; 1 source mean + EF	CCPS (Ref. C5.1), IEEE 493 (Ref. C5.22), NUREG/CR-4639 (Ref. C5.39), NUREG/CR-3831 (Ref. C5.24), NUREG/CR-6890 (Ref. C5.15), NUREG/CR-6928 (Ref. C5.16), SAIC Umatilla (Ref. C5.41), SRS Reactors (Ref. C5.5)
DGS-FTR	Diesel Generator - Seismic - Fails to Run for 29 Days	G	5.05E+01	—	8.27E-04	1 source, N/D	NUREG/CR-6890 (Ref. C5.15)
DM-FOD	Drum Failure on Demand	L	1.00E+01	4.00E-08	—	2 sources mean + EF	EPRI PRA (Ref. C5.8)
DM-MSP	Drum Misspooling (Hourly)	G	5.00E-01	—	6.86E-07	1 source, N/D	NPRD-95 (Ref. C5.40)
DMP-FOH	Damper (Manual) Fails to Operate	L	4.30E+00	—	5.94E-06	3 sources mean + EF	IEEE-500 (Ref. C5.23), N-Reactor (Ref. C5.46), Moss (Ref. C5.32)
DMP-FRO	Damper (Manual) Fails to Remain Open (Transfers Closed)	L	3.20E+00	—	8.38E-08	2 sources N/D; 2 sources mean + EF	NUREG/CR-3154 (Ref. C5.6), NUREG/CR-1363 (Ref. C5.28), NUREG/CR-4639 (Ref. C5.39), SAIC Umatilla (Ref. C5.41)
DMS-FOH	Demister (Moisture Separator) Failure	L	5.00E+00	—	9.12E-06	1 source mean + EF	EPRI AP-2071 (Ref. C5.10)
DRV-FOH	Drive (Adjustable Speed) Failure	G	5.0E-01	—	2.5E-04	1 source; N/D	NPRD-95 (Ref. C5.40)
DRV-FSO	Drive (Adjustable Speed) Failure to Stop on Demand	B	2.5E+02	—	3.4E-05	1 source; N/D	NPRD-95 (Ref. C5.40)
DTC-RUP	Duct Ruptures	L	2.6E+01	—	3.7E-06	9 sources N/D; 1 source mean + EF	NPRD-95 (Ref. C5.40), SRS Reactors (Ref. C5.5), SAIC Umatilla (Ref. C5.41)
DTM-FOD	Damper (Tornado) Failure on Demand	L	5.0E+00	8.7E-04	—	1 source; mean + EF	IEEE-500 (Ref. C5.23)
DTM-FOH	Damper (Tornado) Failure	L	7.9E+00	—	2.3E-05	2 sources N/D; 1 source mean + EF	IEEE-500 (Ref. C5.23), Moss (Ref. C5.32)
ECP-FOH	Position Encoder Failure	G	5.0E-01	—	1.8E-06	2 sources; N/D	NPRD-95 (Ref. C5.40)

Table C4-1. Active Component Reliability Estimates Entered into SAPHIRE Models (Continued)

TYP-FM	Component Name & Failure Mode	Dist Type	Uncertainty Value	Demand Probability	Hourly Failure Rate	Number of Inputs	Input Data Sources ^a
ESC-FOD	Emergency Stop Button Controller Failure to Stop (on Demand)	L	5.0E+00	2.5E-04	—	1 source; mean + EF	EPRI PRA (Ref. C5.8)
FAN-FTR	Fan (Motor-Driven) Fails to Run	L	4.6E+01	—	7.21E-05	11 sources N/D; 6 sources mean + EF	CCPS (Ref. C5.1), N-Reactor (Ref. C5.46), NPRD-95 (Ref. C5.40), NUREG/CR-4639 (Ref. C5.39), NUREG/CR-6928 (Ref. C5.16), SAIC Umatilla (Ref. C5.41), SRS Reactors (Ref. C5.5)
FAN-FTS	Fan (Motor-Driven) Fails to Start on Demand	L	1.0E+01	2.0E-03	—	7 sources N/D; 5 sources mean + EF	CCPS (Ref. C5.1), N-Reactor (Ref. C5.46), NPRD-95 (Ref. C5.40), NUREG/CR-4639 (Ref. C5.39), NUREG/CR-6928 (Ref. C5.16), SAIC Umatilla (Ref. C5.41), SRS Reactors (Ref. C5.5)
FRK-PUN	Forklift Puncture	L	1.06E+01	—	1.20E-05	1 source mean + EF	SAIC Umatilla (Ref. C5.41)
G65-FOH	Governor Failure	G	1.82E+02	—	1.16E-05	1 source; N/D	NPRD-95 (Ref. C5.40)
GPL-FOD	Grapple Failure on Demand	B	1.30E+06	1.15E-06	—	1 source; N/D	NPRD-95 (Ref. C5.40)
GRB-FOH	Gear Box Failure	L	1.40E+01	—	2.21E-04	1 source N/D; 1 source mean + EF	NPRD-95 (Ref. C5.40)
GRB-SHH	Gear box Shaft/Coupling Shears	L	5.00E+00	—	2.40E-06	1 source; mean + EF	EPRI PRA (Ref. C5.8)
GRB-STH	Gear Box Stripped	L	5.00E+00	—	7.86E-08	1 source; mean + EF	NPRD-95 (Ref. C5.40)
HC-FOD	Hand Held Radio Remote Controller Failure to Stop (on Demand)	L	8.39E+01	1.74E-03	—	1 source N/D; 3 sources mean + EF	EPRI PRA (Ref. C5.8), NPRD-95 (Ref. C5.40)
HC-SPO	Hand Held Radio Remote Controller Spurious Operation	G	5.00E-01	—	5.23E-07	1 source N/D	NPRD-95 (Ref. C5.40)
HEP-LEK	Filter (HEPA) Leaks (Bypassed)	L	1.00E+01	—	3.00E-06	1 source; mean + EF	SRS Reactors (Ref. C5.5)

Table C4-1. Active Component Reliability Estimates Entered into SAPHIRE Models (Continued)

TYP-FM	Component Name & Failure Mode	Dist Type	Uncertainty Value	Demand Probability	Hourly Failure Rate	Number of Inputs	Input Data Sources ^a
HEP-PLG	Filter (HEPA) Plugs	L	9.5E+00	—	4.3E-06	3 sources N/D; 2 sources mean + EF	IEEE-500 (Ref. C5.23), NUREG/CR-4639 (Ref. C5.39), SAIC Umatilla (Ref. C5.41)
HOS-LEK	Hose Leaking	L	2.47E+01	—	1.48E-05	same as HOS-RUP with factor of 10	CCPS (Ref. C5.1), NPRD-95 (Ref. C5.40), SAIC Umatilla (Ref. C5.41), SRS Reactors (Ref. C5.5)
HOS-RUP	Hose Ruptures	L	2.47E+01	—	1.48E-06	2 sources N/D; 3 sources mean + EF	CCPS (Ref. C5.1), NPRD-95 (Ref. C5.40), SAIC Umatilla (Ref. C5.41), SRS Reactors (Ref. C5.5)
IEL-FOD	Interlock Failure on Demand	L	5.0E+00	2.8E-05	—	1 source; mean + EF	NPRD-95 (Ref. C5.40)
IEL-FOH	Interlock Failure	L	5.50E+01	—	3.43E-05	4 sources; N/D	NPRD-95 (Ref. C5.40)
LC-FOD	Level Controller Failure on Demand	B	6.07E+03	6.25E-04	—	1 source; N/D	NUREG/CR-6928 (Ref. C5.16)
LRG-FOH	Lifting Rig or Hook Failure	G	4.65E+01	—	7.45E-07	1 source; N/D	NPRD-95 (Ref. C5.40)
LVR-FOH	Lever (two position; up-down) Failure	G	9.85E+01	—	2.10E-06	1 source; N/D	NPRD-95 (Ref. C5.40)
MCC-FOH	Motor Control Centers (MCCs) Failure	L	1.00E+01	—	7.49E-06	composite of Relay (RLY-FTP) + Motor Starter (MST FOH) + Limit Switch (ZS-FOH)	
MOE-FOD	Motor (Electric) Fails on Demand	L	5.00E+00	6.00E-05	—	1 source; mean + EF	EPRI PRA (Ref. C5.8)
MOE-FSO	Motor (Electric) Fails to Shut Off	L	1.07E+01	—	1.35E-08	1 source N/D; 1 source mean + EF	CCPS (Ref. C5.1), MIL-HDBK- 217F (Ref. C5.12)
MOE-FTR	Motor (Electric) Fails to Run	L	9.50E+00	—	6.50E-06	8 sources N/D; 2 sources mean + EF	NPRD-95 (Ref. C5.40), NSWC- 98-LE1 (Ref. C5.37), NUREG/CR-4639 (Ref. C5.39), OREDA-2002 (Ref. C5.43)
MOE-FTS	Motor (Electric) Fails to Start (Hourly)	L	1.90E+01	—	7.14E-06	5 sources N/D; 2 sources mean + EF	NPRD-95 (Ref. C5.40)
MOE-SPO	Motor (Electric) Spurious Operation	L	1.07E+01	—	6.74E-07	1 source N/D; 1 source mean + EF	CCPS (Ref. C5.1), MIL-HDBK- 217F (Ref. C5.12)

Table C4-1. Active Component Reliability Estimates Entered into SAPHIRE Models (Continued)

TYP-FM	Component Name & Failure Mode	Dist Type	Uncertainty Value	Demand Probability	Hourly Failure Rate	Number of Inputs	Input Data Sources ^a
MOH-FOH	Motor (Hydraulic) Failure	G	5.00E-01	—	2.50E-04	1 source; N/D	NPRD-95 (Ref. C5.40)
MSC-FOH	Motor Speed Control Module Failure	G	5.00E-01	—	1.28E-04	1 source; N/D	NPRD-95 (Ref. C5.40)
MST-FOH	Motor Starter Failure	L	1.33E+00	—	1.43E-07	2 sources; N/D	IEEE 493 (Ref. C5.22)
NZL-FOH	Nozzle Failure	L	7.50E+00	—	2.85E-06	5 sources N/D; 1 source mean + EF	IEEE-500 (Ref. C5.23), NPRD-95 (Ref. C5.40), SAIC Umatilla (Ref. C5.41)
PIN-BRK	Pin (Locking or Stabilization) Breaks	L	1.46E+00	—	2.12E-09	4 sources; N/D	NPRD-95 (Ref. C5.40)
PLC-FOD	Programmable Logic Controller Fails on Demand	B	1.35E+03	3.69E-04	—	1 source; N/D	NPRD-95 (Ref. C5.40)
PLC-FOH	Programmable Logic Controller Fails to Operate	L	1.00E+01	—	3.26E-06	5 sources N/D; 1 source mean + EF	MIL-HDBK-217F (Ref. C5.12), NPRD-95 (Ref. C5.40), SAIC Umatilla (Ref. C5.41)
PLC-SPO	Programmable Logic Controller Spurious Operation	L	1.00E+01	—	3.65E-07	5 sources N/D; 1 source mean + EF	MIL-HDBK-217F (Ref. C5.12), NPRD-95 (Ref. C5.40), SAIC Umatilla (Ref. C5.41)
PMD-FTR	Pump (Motor Driven) Fails to Run	L	9.9E+00	—	3.5E-05	6 sources N/D; 87 sources mean + EF	CCPS (Ref. C5.1), N-Reactor (Ref. C5.46), NUREG/CR-4639 (Ref. C5.39), NUREG/CR-1205 (Ref. C5.45), NUREG/CR-2886 (Ref. C5.13), NUREG/CR-6928 (Ref. C5.16), OREDA-2002 (Ref. C5.43), SAIC Umatilla (Ref. C5.41), SRS Reactors (Ref. C5.5)
PMD-FTS	Pump (Motor Driven) Fails to Start on Demand	L	3.80E+00	2.50E-03	—	7 sources N/D; 80 sources mean + EF	N-Reactor (Ref. C5.46), NUREG/CR-4639 (Ref. C5.39), NUREG/CR-1205 (Ref. C5.45), NUREG/CR-2886 (Ref. C5.13), NUREG/CR-6928 (Ref. C5.16), OREDA-2002 (Ref. C5.43), SAIC Umatilla (Ref. C5.41), SRS Reactors (Ref. C5.5)
PPL-RUP	Piping (Lined) Catastrophic	L	1.50E+01	—	4.42E-07	1 source; mean + EF	CCPS (Ref. C5.1)

Table C4-1. Active Component Reliability Estimates Entered into SAPHIRE Models (Continued)

TYP-FM	Component Name & Failure Mode	Dist Type	Uncertainty Value	Demand Probability	Hourly Failure Rate	Number of Inputs	Input Data Sources ^a
PPM-PLG	Piping (Water) Plugs	L	1.35E+01	—	7.26E-07	1 source N/D; 2 sources mean + EF	du Pont (Ref. C5.14), EPRI Pipe Failure Study (Ref. C5.10), SAIC Umatilla (Ref. C5.41)
PPM-RUP	Piping (Water) Ruptures	L	2.00E+01	—	8.75E-10	1 source; mean + EF	NUREG/CR-6928 (Ref. C5.16)
PR-FOH	Passive restraint (bumper) Failure	G	2.09E+02	—	4.45E-10	1 source; N/D	NPRD-95 (Ref. C5.40)
PRM-FOH	EPROM (HVAC Speed Control) Failure	G	5.00E-01	—	5.38E-07	1 source; N/D	MIL-HDBK-217F (Ref. C5.12)
PRV-FOD	Pressure Relief Valve Fails on Demand	L	2.72E+01	6.54E-03	—	6 sources N/D; 2 sources mean + EF	CCPS (Ref. C5.1), NUREG/CR-4639 (Ref. C5.39), NUREG/CR-6928 (Ref. C5.16)
PV-SPO	Pneumatic Valve Spurious Operation	G	5.00E-01	—	2.92E-05	1 source; N/D	NPRD-95 (Ref. C5.40)
QDV-FOH	Quick Disconnect Valve Failure	L	3.56E+00	—	4.26E-06	4 sources N/D	NPRD-95 (Ref. C5.40)
RCV-FOH	Air Receiver Fails to Supply Air	L	1.00E+01	—	6.00E-07	1 source; mean + EF	IEEE-500 (Ref. C5.23)
RLY-FTP	Relay (Power) Fails to Close/Open	G	5.00E-01	—	8.77E-06	1 source N/D	NPRD-95 (Ref. C5.40)
SC-FOH	Speed Control Failure	G	5.00E-01	—	1.28E-04	1 source N/D	NPRD-95 (Ref. C5.40)
SC-SPO	Speed Control Spurious Operation	G	5.00E-01	—	3.20E-05	1 source N/D	NPRD-95 (Ref. C5.40)
SEL-FOH	Speed Selector Fails	L	5.34E+00	—	4.16E-06	3 sources N/D	NPRD-95 (Ref. C5.40)
SEQ-FOD	Sequencer Fails on Demand	B	7.49E+02	3.33E-03	—	1 source N/D	NUREG/CR-6928 (Ref. C5.16)
SFT-COL	Spent Fuel Transfer Machine (SFTM) Collision or Impact	L	4.00E+00	2.94E-06	—	2 sources N/D	NUREG-1774 (Ref. C5.26), McKenna (Ref. C5.20)
SFT-DRP	Spent Fuel Transfer Machine (SFTM) Drop	L	3.00E+00	5.15E-06	—	2 sources N/D	NUREG-1774 (Ref. C5.26), McKenna (Ref. C5.20)
SFT-RTH	Spent Fuel Transfer Machine (SFTM) Raised Fuel Too High	L	7.00E+00	7.36E-07	—	2 sources N/D	NUREG-1774 (Ref. C5.26), McKenna (Ref. C5.20)
SJK-FOH	Screw Jack (TEV) Failure	G	5.00E-01	—	8.14E-06	1 source; N/D	NPRD-95 (Ref. C5.40)

Table C4-1. Active Component Reliability Estimates Entered into SAPHIRE Models (Continued)

TYP-FM	Component Name & Failure Mode	Dist Type	Uncertainty Value	Demand Probability	Hourly Failure Rate	Number of Inputs	Input Data Sources ^a
SRF-FOH	Flow Sensor Failure	G	5.00E-01	—	1.07E-06	1 source; N/D	NUREG/CR-4639 (Ref. C5.39)
SRP-FOD	Pressure Sensor Fails on Demand	B	1.25E+02	3.99E-03	—	1 source; N/D	NPRD-95 (Ref. C5.40)
SRP-FOH	Pressure Sensor Fails	L	1.21E+01	—	2.95E-06	8 sources N/D	NPRD-95 (Ref. C5.40), NUREG/CR-6928 (Ref. C5.16)
SRR-FOH	Radiation Sensor Fails	L	5.00E+00	—	2.00E-05	1 source; mean + EF	Laurus (Ref. C5.25)
SRS-FOH	OverSpeed Sensor Fails	G	1.28E+02	—	2.14E-05	1 source; N/D	NPRD-95 (Ref. C5.40)
SRT-FOD	Temperature Sensor/Transmitter Fails on Demand	L	2.10E+00	7.33E-04	—	2 sources N/D	NUREG/CR-6928 (Ref. C5.16), OREDA-92 (Ref. C5.42)
SRT-FOH	Temperature Sensor/Transmitter Fails	L	1.41E+01	—	7.05E-07	4 sources N/D; 2 sources mean + EF	NPRD-95 (Ref. C5.40), NUREG/CR-6928 (Ref. C5.16), OREDA-2002 (Ref. C5.43)
SRT-SPO	Temperature Sensor Spurious Operation	L	2.80E+01	—	2.23E-06	1 source; mean + EF	OREDA-2002 (Ref. C5.43)
SRU-FOH	Ultrasonic Sensor Fails	G	5.00E-01	—	9.62E-05	1 source; N/D	NPRD-95 (Ref. C5.40)
SRV-FOH	Vibration Sensor (Accelerometer) Fails	L	1.07E+01	—	9.40E-05	4 sources N/D	NPRD-95 (Ref. C5.40)
SRX-FOD	Optical Position Sensor Fails on Demand	B	3.18E+03	1.10E-03	—	1 source; N/D	SAIC Umatilla (Ref. C5.41)
SRX-FOH	Optical Position Sensor Fails	L	5.00E+00	—	4.70E-06	1 source; mean + EF	NPRD-95 (Ref. C5.40)
STR-FOH	Steering (tractor or trailer) Fails	L	4.63E+01	—	1.84E-05	4 sources N/D	NPRD-95 (Ref. C5.40)
STU-FOH	Structure (truck or railcar) Failure	G	1.50E+00	—	4.81E-08	1 source; N/D	NPRD-95 (Ref. C5.40)
SV-FOD	Solenoid Valve Fails on Demand	L	1.17E+01	6.28E-04	—	4 sources N/D; 5 sources mean + EF	CCPS (Ref. C5.1), N-Reactor (Ref. C5.46), NSW-98-LE1 (Ref. C5.37), NUREG/CR-4639 (Ref. C5.39), NUREG/CR-6928 (Ref. C5.16), SRS Reactors (Ref. C5.5)

Table C4-1. Active Component Reliability Estimates Entered into SAPHIRE Models (Continued)

TYP-FM	Component Name & Failure Mode	Dist Type	Uncertainty Value	Demand Probability	Hourly Failure Rate	Number of Inputs	Input Data Sources ^a
SV-FOH	Solenoid Valve Fails	L	1.70E+01	—	4.87E-05	1 source; mean + EF	CCPS (Ref. C5.1)
SV-SPO	Solenoid Valve Spurious Operation	L	3.00E+00	—	4.09E-07	1 source; mean + EF	CCPS (Ref. C5.1)
SWA-FOH	Auto-Stop Switch (CTT hose travel) Fails	G	6.50E+00	—	3.12E-06	1 source; N/D	NPRD-95 (Ref. C5.40)
SWG-FOH	13.8kV Switchgear Fails	G	2.85E+01	—	1.31E-07	1 source; N/D	IEEE 493 (Ref. C5.22)
SWP-FTX	Electric Power Switch Fails to Transfer	G	6.50E+00	—	3.59E-07	1 source; N/D	IEEE 493 (Ref. C5.22)
SWP-SPO	Electric Power Switch Spurious Transfer	G	6.50E+00	—	1.55E-07	1 source; N/D	IEEE 493 (Ref. C5.22)
TD-FOH	Transducer Failure	L	4.70E+00	—	9.84E-05	3 sources N/D; 1 source mean + EF	NPRD-95 (Ref. C5.40)
TDA-FOH	Transducer (Air Flow) Failure	L	6.21E+00	—	1.65E-04	2 sources N/D	NPRD-95 (Ref. C5.40), NSWC-98-LE1 (Ref. C5.37)
TDP-FOH	Transducer (Pressure) Fails	L	5.35E+01	—	2.20E-04	23 sources N/D; 2 sources mean + EF	NPRD-95 (Ref. C5.40), NSWC-98-LE1 (Ref. C5.37)
TDT-FOH	Transducer (Temperature) Fails	L	2.95E+01	—	1.04E-04	12 sources N/D; 1 source mean + EF	NPRD-95 (Ref. C5.40)
THR-BRK	Third Rail Breaks	L	1.00E+01	—	1.01E-08	1 source; mean + EF	NPRD-95 TRK-BRK adjusted with failure information from Federal Railroad Administration Safety Data website (Ref. C5.17)
TKF-FOH	Fuel Tank Fails	L	1.11E+01	—	4.40E-07	15 sources; N/D	NPRD-95 (Ref. C5.40), NUREG/CR-4639 (Ref. C5.39), NUREG/CR-6928 (Ref. C5.16)
TL-FOH	Torque Limiter Failure	G	8.05E+01	—	8.05E-05	1 source N/D	NPRD-95 (Ref. C5.40)
TRD-FOH	Tread (Site Transporter)	L	3.40E+00	—	5.89E-07	1 source N/D; 1 source mean + EF	NPRD-95 (Ref. C5.40), Rand (Ref. C5.38)
UDM-FOH	Damper (Backdraft) Failure	L	7.90E+00	—	2.26E-05	2 sources N/D; 1 source mean + EF	IEEE-500 (Ref. C5.23), Moss (Ref. C5.32)

Table C4-1. Active Component Reliability Estimates Entered into SAPHIRE Models (Continued)

TYP-FM	Component Name & Failure Mode	Dist Type	Uncertainty Value	Demand Probability	Hourly Failure Rate	Number of Inputs	Input Data Sources ^a
UPS-FOH	Uninterruptible Power Supply (UPS) Failure	L	5.08E+00	—	2.02E-06	10 sources; N/D	NPRD-95 (Ref. C5.40)
WNE-BRK	Wire Rope Breaks	L	5.00E+00	2.00E-06	—	1 source; mean + EF	EPRI PRA (Ref. C5.8)
XMR-FOH	Transformer Failure	L	1.53E+01	—	2.91E-07	13 sources N/D; 2 sources mean + EF	CCPS (Ref. C5.1), MIL-HDBK-217F (Ref. C5.12), NPRD-95 (Ref. C5.40), NUREG/CR-4639 (Ref. C5.39), NUREG/CR-6928 (Ref. C5.16)
XV-FOD	Manual Valve Failure on Demand	L	1.00E+01	6.48E-04	—	3 sources N/D; 12 sources mean + EF	CCPS (Ref. C5.1), N-Reactor (Ref. C5.46), NUREG/CR-4639 (Ref. C5.39), NUREG/CR-6928 (Ref. C5.16), SRS Reactors (Ref. C5.5)
ZS-FOD	Limit Switch Failure on Demand	L	5.7E+00	2.9E-04	—	3 sources N/D	MIL-HDBK-217F (Ref. C5.12), NPRD-95 (Ref. C5.40), SRS Reactors (Ref. C5.5)
ZS-FOH	Limit Switch Fails	L	6.03E+00	—	7.23E-06	3 sources N/D	MIL-HDBK-217F (Ref. C5.12), NPRD-95 (Ref. C5.40), NUREG/CR-4639 (Ref. C5.39)
ZS-SPO	Limit Switch Spurious Operation	L	5.56E+00	—	1.28E-06	3 sources N/D	MIL-HDBK-217F (Ref. C5.12), NPRD-95 (Ref. C5.40), NUREG/CR-4639 (Ref. C5.39)

NOTE: ^a Refer to Section C1.2 for specific citation to data sources.

B = beta distribution; Dist Type = Distribution Type; EPROM = erasable programmable read-only memory; EF = Lognormal Error Factor; G = gamma distribution; L = lognormal distribution; N/D = Numerator/Denominator; TYP-FM = Component Type and Failure Mode.

Source: Original

C5 REFERENCES; DESIGN INPUTS

The PCSA is based on a snapshot of the design. The reference design documents are appropriately documented as design inputs in this section. Since the safety analysis is based on a snapshot of the design, referencing subsequent revisions to the design documents (as described in EG-PRO-3DP-G04B-00037, *Calculations and Analyses* (Ref. 2.1.1, Section 3.2.2.F)) that implement PCSA requirements flowing from the safety analysis would not be appropriate for the purpose of the PCSA.

The inputs in this Section noted with an (*) indicate that they fall into one of the designated categories described in Section 4.1, relative to suitability for intended use.

- C5.1 *AIChE (American Institute of Chemical Engineers) 1989. *Guidelines for Process Equipment Reliability Data with Data Tables*. G-07. New York, New York: American Institute of Chemical Engineers, Center for Chemical Process Safety. TIC: 259872. ISBN: 978-0-8169-0422-8.
- C5.2 *Apostolakis, G. and Kaplan, S. 1981. "Pitfalls in Risk Calculations." *Reliability Engineering*, 2, 135-145. Barking, England: Applied Science Publishers. TIC: 253648.
- C5.3 ASME NOG-1-2004. 2005. *Rules for Construction of Overhead and Gantry Cranes (Top Running Bridge, Multiple Girder)*. New York, New York: American Society of Mechanical Engineers. TIC: 257672. ISBN: 0-7918-2939-1.
- C5.4 *Atwood, C.L.; LaChance, J.L.; Martz, H.F.; Anderson, D.J.; Englehardt, M.; Whitehead, D.; and Wheeler, T. 2003. *Handbook of Parameter Estimation for Probabilistic Risk Assessment*. NUREG/CR-6823. Washington, D.C.: U.S. Nuclear Regulatory Commission. ACC: MOL.20060126.0121.
- C5.5 *Blanton, C.H. and Eide, S.A. 1993. *Savannah River Site, Generic Data Base Development (U)*. WSRC-TR-93-262. Aiken, South Carolina: Westinghouse Savannah River Company. TIC: 246444.
- C5.6 *Borkowski, R.J.; Kahl, W.K.; Hebble, T.L.; Fragola, J.R.; Johnson, J.W. 1983. *The In-Plant Reliability Data Base for Nuclear Plant Components: Interim Report-The Valve - Component*. NUREG/CR-3154; ORNL/TM-8647. Oak Ridge, TN: Oak Ridge National Laboratory. ACC: MOL.20071129.0315.
- C5.7 BSC 2007 (Bechtel SAIC Company). *Waste Form Throughputs for Preclosure Safety Analysis*. 000-PSA-MGR0-01800-000-00A. Las Vegas, Nevada: Bechtel SAIC Company. ACC: ENG.20071106.0001.
- C5.8 *Canavan, K.; Gregg, B.; Karimi, R.; Mirsky, S.; and Stokley, J. 2004. *Probabilistic Risk Assessment (PRA) of Bolted Storage Casks, Updated Quantification and Analysis Report*. 1009691. Palo Alto, California: Electric Power Research Institute. TIC: 257542.

- C5.9 *Crutchfield, D.M. 1996. "Movement of Heavy Loads Over Spent Fuel, Over Fuel in the Reactor Core, or Over Safety-Related Equipment." NRC Bulletin 96-02. Washington, D.C.: U.S. Nuclear Regulatory Commission. Accessed February 12, 2008. ACC: MOL.20080213.0021. URL: <http://www.nrc.gov/reading-rm/doc-collections/gen-comm/bulletins/1996/b196002.html>
- C5.10 *Derdiger, J.A.;Bhatt, K.M.;Siegfriedt, W.E. 1981. *Component Failure and Repair Data for Coal-Fired Power Units*. EPRI AP-2071. Palo Alto, CA: Electric Power Research Institute. TIC: 260070.
- C5.11 *Dhillon, B.S. 1988. *Mechanical Reliability: Theory, Models and Applications*. AIAA Education Series. Washington, D.C.: American Institute of Aeronautics & Astronautics. TIC: 259878.
- C5.12 *DOD (U.S. Department of Defense) 1991. *Military Handbook, Reliability Prediction of Electronic Equipment*. MIL-HDBK-217F. Washington, D.C.: U.S. Department of Defense. TIC: 232828.
- C5.13 *Drago, J.P.; Borkowski, R.J.; Fragola, J.R.; and Johnson, J.W. 1982. *The In-Plant Reliability Data Base for Nuclear Plant Components: Interim Data Report — The Pump Component*. NUREG/CR-2886. Washington, D.C.: U.S. Nuclear Regulatory Commission. ACC: MOL.20071219.0222.
- C5.14 *E.I. du Pont de Nemours & Company. 1981. *Some Published and Estimated Failure Rates for Use in Fault Tree Analysis*. Wilmington, Delaware: E.I. du Pont de Nemours & Company. TIC: 260092. (DIRS 184415)
- C5.15 *Eide, S.A.; Gentillon, C.D.; Wierman, T.E.; and Rasmuson, D.M. 2005. *Analysis of Station Blackout Risk*. Volume 2 of *Reevaluation of Station Blackout Risk at Nuclear Power Plants*. NUREG/CR-6890. Washington, D.C.: U.S. Nuclear Regulatory Commission. ACC: MOL.20071114.0165.
- C5.16 *Eide, S.A.; Wierman, T.E.; Gentillon, C.D.; Rasmuson, D.M.; and Atwood, C.T. 2007. *Industry-Average Performance for Components and Initiating Events at U.S. Commercial Nuclear Power Plants*. NUREG/CR-6928. Washington, D.C.: U.S. Nuclear Regulatory Commission. ACC: MOL.20071211.0229.
- C5.17 *Federal Railroad Administration. 2004. "Train Accidents by Cause from Form FRA F 6180.54." Washington, D.C.: U.S. Department of Transportation, Federal Railroad Administration. Accessed 03/12/2004. ACC: MOL.20040311.0211. URL: <http://safetydata.fra.dot.gov/OfficeofSafety/Query/Default.asp>
- C5.18 *Fleming, K.N. 1975. *A Reliability Model for Common Mode Failures in Redundant Safety Systems*. GA-A13284. San Diego, California: General Atomic Company. ACC: MOL.20071219.0221.

- C5.19 *Fragola, J.R. and McFadden, R.H. 1995. "External Maintenance Rate Prediction and Design Concepts for High Reliability and Availability on Space Station Freedom." *Reliability Engineering and System Safety*, 47, 255-273. New York, New York: Elsevier. TIC: 259675.
- C5.20 *Framatome ANP (Advanced Nuclear Power) 2001. *Summary, Commercial Nuclear Fuel Assembly Damage/Misload Study – 1985-1999*. Lynchburg, Virginia: Framatome Advanced Nuclear Power. ACC: MOL.20011018.0158.
- C5.21 *HID Corporation [n.d.]. *Ruggedized Card Reader/Ruggedized Keypad Card Reader. Dorado 740 and 780*. Irvine, California: HID Corporation. TIC: 260007.
- C5.22 *IEEE (Institute of Electrical and Electronics Engineers) Std 493-1997. 1998. *IEEE Recommended Practice for the Design of Reliable Industrial and Commercial Power Systems*. New York, New York: Institute of Electrical and Electronics Engineers. TIC: 243205. ISBN: 1-55937-969-3.
- C5.23 *IEEE Std 500-1984 (Reaffirmed 1991). 1991. *IEEE Guide to the Collection and Presentation of Electrical, Electronic, Sensing Component, and Mechanical Equipment Reliability Data for Nuclear-Power Generating Stations*. New York, New York: Institute of Electrical and Electronics Engineers. TIC: 256281.
- C5.24 *Kahl, W.K. and Borkowski, R.J. 1985. *The In-Plant Reliability Data Base for Nuclear Plant Components: Interim Report - Diesel Generators, Batteries, Chargers, and Inverters*. NUREG/CR-3831. Washington, D.C.: U.S. Nuclear Regulatory Commission. ACC: MOL.20071212.0181.
- C5.25 *Laurus Systems [n.d.]. *Instruments and Software Solutions for Emergency Response and Health Physics*. Ellicott City, Maryland: Laurus Systems. TIC: 259965.
- C5.26 Lloyd, R.L. 2003. *A Survey of Crane Operating Experience at U.S. Nuclear Power Plants from 1968 through 2002*. NUREG-1774. Washington, D.C.: U.S. Nuclear Regulatory Commission. ACC: MOL.20050802.0185.
- C5.27 *Lopez Droguett, E.; Groen, F.; and Mosleh, A. 2004. "The Combined Use of Data and Expert Estimates in Population Variability Analysis." *Reliability Engineering and System Safety*, 83, 311-321. New York, New York: Elsevier. TIC: 259380.
- C5.28 *Miller, C.F.; Hubble, W.H.; Trojovsky, M.; and Brown, S.R. 1982. *Data Summaries of Licensee Event Reports of Valves at U.S. Commercial Nuclear Power Plants from January 1, 1976 to December 31, 1980*. NUREG/CR-1363, Rev. 1. Washington, D.C.: U.S. Nuclear Regulatory Commission. ACC: MOL.20071219.0223.
- C5.29 *Mosleh, A.; Fleming, K.N.; Parry, G.W.; Paula, H.M.; Worledge, D.H.; and Rasmuson, D.M. 1988. *Analytical Background and Techniques. Volume 2 of Procedures for Treating Common Cause Failures in Safety and Reliability Studies*. NUREG/CR-4780. Washington, D.C.: U.S. Nuclear Regulatory Commission. TIC: 221775.

- C5.30 *Mosleh, A.; Fleming, K.N.; Parry, G.W.; Paula, H.M.; Worledge, D.H.; and Rasmuson, D.M. 1988. *Procedural Framework and Examples*. Volume 1 of *Procedures for Treating Common Cause Failures in Safety and Reliability Studies*. NUREG/CR-4780. Washington, D.C.: U.S. Nuclear Regulatory Commission. TIC: 221775.
- C5.31 *Mosleh, A.; Rasmuson, D.M.; and Marshall, F.M. 1998. *Guidelines on Modeling Common-Cause Failures in Probabilistic Risk Assessment*. NUREG/CR-5485. Washington, D.C.: U.S. Nuclear Regulatory Commission. ACC: MOL.20040220.0106.
- C5.32 *Moss, T.R. 2005. *The Reliability Data Handbook*. 1st Edition. New York, New York: ASME Press (American Society of Mechanical Engineers). ISBN: 0-7918-0233-7. TIC: 259912.
- C5.33 Not used.
- C5.34 NRC (U.S. Nuclear Regulatory Commission) 1979. *Single-Failure-Proof Cranes for Nuclear Power Plants*. NUREG-0554. Washington, D.C.: U.S. Nuclear Regulatory Commission. TIC: 232978.
- C5.35 NRC 1980. *Control of Heavy Loads at Nuclear Power Plants*. NUREG-0612. Washington, D.C.: U.S. Nuclear Regulatory Commission. TIC: 209017.
- C5.36 NRC 2005. *CCF Parameter Estimation 2005*. Washington, D.C.: Nuclear Regulatory Commission (NRC). ACC: MOL.20080213.0022.
- C5.37 *NSWC (Naval Surface Warfare Center) 1998. *Handbook of Reliability Prediction Procedures for Mechanical Equipment*. NSWC-98/LE1. West Bethesda, Maryland: Naval Surface Warfare Center, Carderock Division. TIC: 245703.
- C5.38 *Peltz, E.; Robbins, M.; Boren, P.; Wolff, M. 2002. "Using the EDA to Gain Insight into Failure Rates." *Diagnosing the Army's Equipment Readiness: The Equipment Downtime Analyzer*. Santa Monica, CA: RAND. TIC: 259917. ISBN: 0-8330-3115-5.
- C5.39 *Reece, W.J.; Gilbert, B.G.; and Richards, R.E. 1994. *Nuclear Computerized Library for Assessing Reactor Reliability (NUCLARR), Volume 5: Data Manual, Part 3: Hardware Component Failure Data*. NUREG/CR-4639, Vol. 5, Rev. 4. Washington, D.C.: U.S. Nuclear Regulatory Commission. ACC: MOL.20071220.0209.
- C5.40 *Denson, W.; Chandler, G.; Crowell, W.; Clark, A.; and Jaworski, P. 1994. *Nonelectronic Parts Reliability Data 1995*. NPRD-95. Rome, New York: Reliability Analysis Center. TIC: 259757.
- C5.41 *SAIC (Science Applications International Corporation) 2002. *Umatilla Chemical Agent Disposal Facility Quantitative Risk Assessment*. Report No. SAIC-00/2641. Volume I. Abingdon, Maryland: Science Applications International Corporation. ACC: MOL.20071220.0210.

- C5.42 *SINTEF Industrial Management 1992. *OREDA, Offshore Reliability Data Handbook*. 2nd Edition. Trondheim, Norway: OREDA. ISBN: 825150188.1
- C5.43 *SINTEF Industrial Management 2002. *OREDA, Offshore Reliability Data Handbook*. 4th Edition. Trondheim, Norway: OREDA. ISBN: 8214027055. TIC: 257402.
- C5.44 *Siu, N.O. and Kelly, D.L. 1998. "Bayesian Parameter Estimation in Probabilistic Risk Assessment." *Reliability Engineering and System Safety*, 62, 89-116. New York, New York: Elsevier. TIC: 258633.
- C5.45 *Trojovsky, M. 1982. *Data Summaries of Licensee Event Reports of Pumps at U.S. Commercial Nuclear Power Plants, January 1, 1972 to April 30, 1980*. NUREG/CR-1205, Rev. 1. Washington, D.C.: U.S. Nuclear Regulatory Commission. ACC: MOL.20080207.0024.
- C5.46 *Zentner, M.D.; Atkinson, J.K.; Carlson, P.A.; Coles, G.A.; Leitz, E.E.; Lindberg, S.E.; Powers, T.B.; and Kelly, J.E. 1988. *N Reactor Level 1 Probabilistic Risk Assessment: Final Report*. WHC-SP-0087. Richland, Washington: Westinghouse Hanford Company. ACC: MOL.20080207.0021.

ATTACHMENT D
PASSIVE EQUIPMENT FAILURE ANALYSIS

INTENTIONALLY LEFT BLANK

CONTENTS

	Page
ACRONYMS AND ABBREVIATIONS	D-7
D1 LOSS OF CONTAINMENT DUE TO DROPS AND IMPACTS	D-9
D1.1 LAWRENCE LIVERMORE NATIONAL LABORATORY ANALYSIS OF CANISTERS AND CASKS	D-10
D1.2 IDAHO NATIONAL LABORATORY ANALYSIS OF SPENT NUCLEAR FUEL CANISTERS AND MULTICANISTER OVERPACKS	D-14
D1.3 PROBABILITIES OF FAILURE OF HIGH LEVEL WASTE CANISTERS DUE TO DROPS	D-21
D1.4 PROBABILITIES OF FAILURE OF WASTE PACKAGES DUE TO DROPS AND IMPACTS	D-23
D1.5 PREDICTING OUTCOMES OF OTHER SITUATIONS BY EXTRAPOLATING STRAINS FOR MODELED SCENARIOS	D-28
D1.6 MISCELLANEOUS SCENARIOS	D-30
D2 PASSIVE FAILURE DUE TO FIRE	D-31
D2.1 ANALYSIS OF CANISTER FAILURE DUE TO FIRE	D-32
D2.2 SHIELDING DEGRADATION IN A FIRE	D-71
D3 SHIELDING DEGRADATION DUE TO IMPACTS	D-74
D3.1 DAMAGE THRESHOLDS FOR LOS	D-76
D3.2 SEVERITY OF DAMAGE VERSUS IMPACT VELOCITY	D-77
D3.3 ESTIMATE OF THRESHOLD SPEEDS FOR LOSS OF SHIELDING DUE TO IMPACTS	D-81
D3.4 PROBABILITY OF LOSS OF SHIELDING	D-83
D4 REFERENCES	D-89
D4.1 DESIGN INPUTS	D-89
D4.2 DESIGN CONSTRAINTS	D-95

INTENTIONALLY LEFT BLANK

FIGURES

	Page
D1.1-1. Original and Shifted Cumulative Distribution Functions (CDF) for Capacity (or Fragility) Plotted as a Function of True Strain.....	D-11
D2.1-1. Comparison Between Results Calculated Using the Simplified Heat Transfer Model and ANSYS – Fire Engulfing a TAD Canister in a Waste Package	D-45
D2.1-2. Plot of Larson-Miller Parameter for Type 316 Stainless Steel	D-56
D2.1-3. Yield, Ultimate, and Flow Stress for Type 316 Stainless Steel	D-57
D2.1-4. Probability Distribution for the Failure Temperature of Thin-Walled Canisters ...	D-61
D2.1-5. Probability Distribution for the Failure Temperature of Thick-Walled Canisters.....	D-62
D2.1-6. Probability Distribution for Maximum Canister Temperature – Thin-Walled Canister in a Waste Package.....	D-64
D2.1-7. Distribution of Radiation Energy from Fire.....	D-70
D3.2-1. Illustration of Deformation and Lead Slumping for a SLS Rail Cask Following End-on Impact at 120 mph	D-79
D3.2-2. Truck Steel/Lead/Steel Inner Shell Strain versus Impact Speed	D-80
D3.2-3. Rail Steel/Lead/Steel Strain versus Impact Speed.....	D-81
D3.4-1. Summary Event Tree Showing Model Logic for Canisters and Aging Overpacks	D-84

TABLES

	Page
D1.1-1. Probability of Failure versus True Strain Tabulated for Figure D1.1-1	D-12
D1.2-1. Container Configurations and Loading Conditions	D-15
D1.2-2. Failure Probabilities with and without Triaxiality Factor, with and without the Fragility Curve Adjustment, for Representative Canister within an Aging Overpack	D-16
D1.2-3. Failure Probabilities with and without Triaxiality Factor, with and without Fragility Curve Adjustment, for Representative Canister	D-17
D1.2-4. Failure Probabilities with and without Triaxiality Factor, with and without the Fragility Curve Adjustment, for the Representative Canister inside the Transportation Cask	D-18
D1.2-5. Failure Probabilities with and without Triaxiality Factor, with and without the Fragility Curve Adjustment, for the Transportation Cask	D-19
D1.2-6. Strains at Various Canister Locations Due to Drops	D-20
D1.2-7. Failure Probabilities for the DOE Spent Nuclear Fuel (DSNF) Canisters and Multicanister Overpack (MCO)	D-21
D1.4-1. Waste Package Probabilities of Failure for Various Drop and Impact Events	D-25
D1.5-1. Calculated Strains and Failure Probabilities for Given Side Impact Velocities	D-29
D2.1-1. Probability Distribution for Fire Duration - Without Automatic Fire Suppression	D-35
D2.1-2. Probability Distribution for Fire Duration - With Automatic Fire Suppression	D-37
D2.1-3. Effective Thermal Properties for 21-PWR Fuel in a TAD	D-41
D2.1-4. Model Inputs – Bare Canister	D-48
D2.1-5. Model Inputs – Canister in a Waste Package	D-49
D2.1-6. Model Inputs – Canister in Transportation Cask	D-50
D2.1-7. Model Inputs – Canister in a Shielded Bell	D-51
D2.1-8. Summary of Canister Failure Probabilities in Fire	D-65
D2.1-9. Model Inputs – Bare Fuel Cask	D-67
D2.1-10. Summary of Fuel Failure Probabilities	D-69
D2.1-11. Probabilities that Radiation Input Exceeds Failure Energy for Cask	D-71
D3.2-1. Maximum Plastic Strain in Inner Shell of Sandwich Wall Casks	D-78
D3.3-1. Drop Height to Reach a Given Impact Speed	D-83
D3.3-2. Impact Speeds on Real Target for Equivalent Damage for Unyielding Targets	D-83
D3.4-1. Probabilities of Degradation or Loss of Shielding	D-88

ACRONYMS AND ABBREVIATIONS

Acronyms

COV	coefficient of variation	
CTM	canister transfer machine	
DOE	U.S. Department of Energy	
DPC	dual-purpose canister	
EPS	equivalent (or effective) plastic strain	
ETF	expended toughness fraction	
FEA	finite element analysis	
HLW	high-level radioactive waste	
INL	Idaho National Laboratory	
LLNL	Lawrence Livermore National Laboratory	
LOS	loss of shielding	
MCO	multicanister overpack	
PCSA	preclosure safety analysis	
SAR	Safety Analysis Report	
SLS	steel-lead-steel	
SNF	spent nuclear fuel	
TAD	transportation, aging, and disposal	
TEV	transport and emplacement vehicle	
WPTT	waste package transfer trolley	

Abbreviations

C	Celsius
cm	centimeter
F	Fahrenheit
ft	foot, feet
hr, hrs	hour, hours
J	joule
K	Kelvin
kg	kilogram
kW	kilowatt
m	meter
min	minute, minutes
MJ	megajoules
m/s	meters/second
mrem	millirem
MPa	megapascal
mph	miles per hour
psig	pounds per square inch gauge
rem	roentgen equivalent man
W/m K	watts per meter Kelvin
W/m ² K	watts per square meter Kelvin

ATTACHMENT D PASSIVE EQUIPMENT FAILURE ANALYSIS

Many event sequences described in Section 6.1 include pivotal events that arise from loss of integrity of a passive component, namely one of the aging overpacks, casks, or canisters that contain a radioactive waste form. Such pivotal events involve (1) loss of containment of radioactive material that may result in airborne releases, or (2) loss of shielding effectiveness. Both types of pivotal events may be failure modes caused by either physical impact to the container or by thermal energy transferred to the container. This attachment presents the results of passive failure analyses that provide conditional probability of loss of containment or loss of shielding. Many scenarios were selected for analysis as representative or bounding for anticipated scenarios in the risk assessment. Results of some scenarios may not have been used in the final event sequence quantification.

D1 LOSS OF CONTAINMENT DUE TO DROPS AND IMPACTS

The category of passive equipment includes canisters and casks used during transport, aging, and disposal of spent nuclear fuel. The canisters and casks contain the spent fuel and provide containment of radioactive material. During transport and handling, the canisters and casks could be subjected to drops, impacts, or fires, which may result in loss of containment. The probabilities of loss of containment due to various physical or thermal challenges are evaluated primarily through structural and thermal analysis and drop test data.

Passive equipment (e.g., transportation casks, storage canisters, and waste packages) may fail from abnormal use such as defined by the event sequences. Studies were performed and passive equipment failure probabilities were determined using the methodologies summarized in Section 4.3.2.2. The probability of loss of containment (breach) was determined for several types of containers, including transportation casks (analyzed without impact limiters), shielded transfer casks, waste packages, transportation, aging, and disposal (TAD) canisters, dual-purpose canisters (DPCs), U.S. Department of Energy (DOE) standardized canisters, multicanister overpacks (MCOs), high-level radioactive waste (HLW) canisters, and naval spent nuclear fuel (SNF) canisters. The mechanical breach of TAD canisters, DPCs and naval SNF canisters were analyzed as representative canisters as described in Section D1.1. The structural analysis of DOE standardized canisters and MCOs for breaches is described in Section D1.2 and then the probabilistic methodology of Section D1.1 was applied. Transportation casks, site transfer casks (STCs) and horizontal STCs were analyzed as representative transportation casks as describe in Section D1.1. The probabilistic estimation of breach from mechanical loads of all other waste containers is described in Sections D1.3 through D1.6. The analysis of loss or degradation of shielding of casks and overpacks against mechanical loads is described in Section D3. The probabilistic analysis of fire severity and the associated effects on casks, canisters, and overpacks with respect to both containment breach and shielding degradation or loss is described in Section D2. The analysis of mechanical failures and thermal failures included the specific configuration defined by the event sequences. For example, if the event sequence occurred during a process in which the canister is within a transportation casks or aging overpack, the analysis is performed in that configuration.

D1.1 LAWRENCE LIVERMORE NATIONAL LABORATORY ANALYSIS OF CANISTERS AND CASKS

Lawrence Livermore National Laboratory (LLNL) performed the finite element analysis (FEA) using Livermore Software–Dynamic Finite Element Program (LS-DYNA) to model drops and impacts for casks and canisters with selected properties for use as representative containers expected to be delivered to Yucca Mountain (Ref. D4.1.27). LS-DYNA, which has been used in nuclear facility and non-nuclear industrial applications, is appropriate to model nonlinear, transient responses of a passive component to a structural challenge such as a drop or an impact. Existing commercial casks and canisters that would likely be used on the Yucca Mountain Project (YMP) were identified and characterized. The cases analyzed are listed in Table D1.2-1.

Appropriate finite element models were developed for the representative cask, selected container types, configurations, and drop types. The level of detail for each model was selected to understand deformation and damage patterns, possible failure mode(s) in each structural element, and failure-related response. Special attention was required to properly model the bottom-weld and closure regions to ensure that coarser mesh of the simplified model would capture failure-related response with acceptable accuracy. A consistent failure criterion for each case was identified as part of the detailed analyses. The effective plastic strain in each element, in combination with material ductility data, was used to predict failure measures.

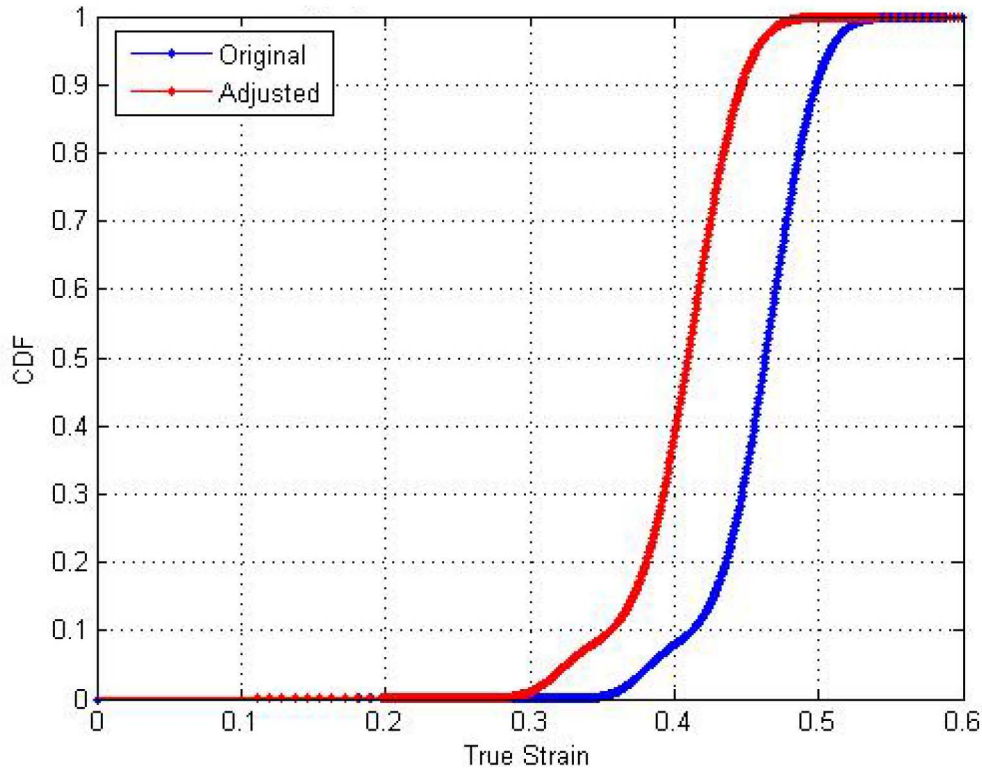
The maximum strain for each scenario was compared with the capacity distribution based on material properties to obtain containment failure probabilities using the methodology described in Section 4.3.2.2. For simplicity and consistency in interpreting results, the impact-surface conditions, including both the ground and the falling 10-ton load for the analyses, were considered infinitely stiff and unyielding, which is conservative.

The results of these cases are summarized in Tables D1.2-2 through D1.2-4. The bases for these results are summarized in the following paragraphs. If a probability for the event sequence is less than 1.0×10^{-8} , additional conservatism is incorporated in the preclosure safety analysis (PCSA) by using a failure probability of 1.0×10^{-5} , which are termed “LLNL, adjusted”. This additional conservatism is added to account for a) future evolutions of cask and canister designs, and b) uncertainties, such as undetected material defects, undetected manufacturing deviations, and undetected damage associated with handling before the container reaches the repository, which are not included in the tensile elongation data.

LLNL developed a fragility curve for the base metal by fitting a mixture of two normal probability density functions to the engineering (tensile) strain data (Ref. D4.1.4). Both the data and their corresponding log-transforms were found to be non-normally distributed ($p < 10^{-4}$) by the Shapiro-Wilk test (Ref. D4.1.62). These data collected at 100°F were determined to be reasonably well modeled as a sample from a weighted mixture of two normal distributions, one with a mean of 46% and a standard deviation of 2.24% (weight = 7.84%), and the other with a mean of 59.3% and a standard deviation of 4.22% (weight = 92.16%), with the goodness of fit ($p = 0.939$) assessed by the Kolmogorov-Smirnov 1 sample test (Ref. D4.1.33).

The stainless steel used in the LLNL (Ref. D4.1.27) analysis is alloy 304L. The un-annealed alloys have relatively shorter elongations at failure than annealed 304L. Therefore, the base

fragility cumulative distribution function model was adjusted to different steels used in a typical design and to meet the code specification of the material model used in LS-DYNA. The adjustment consisted of shifting the distribution by -8.3% (Ref. D4.1.27, p. 93). Thus the initial fragility curve was shifted by 8.3% to a lower value of minimum elongation. The fragility curves, before and after the shift, are shown in Figure D1.1-1 and tabulated in Table D1.1-1. 316L stainless steel might be used for construction of some canisters and casks, but the stress-strain curves would be similar.



Source: Ref. D4.1.27, Figure 6.3.7-3

Figure D1.1-1. Original and Shifted Cumulative Distribution Functions (CDF) for Capacity (or Fragility) Plotted as a Function of True Strain

Table D1.1-1. Probability of Failure versus True Strain Tabulated for Figure D1.1-1

True Strain (TS)	$\frac{TS - TS_{mean}}{TS_{std}}$	Probability of Failure Original	Probability of Failure Adjusted (-8.3% shift)	True Strain (TS)	$\frac{TS - TS_{mean}}{TS_{std}}$	Probability of Failure Original	Probability of Failure Adjusted (-8.3% shift)
0.00	-1.70	0.0000E+00	1.6754E-15	0.36	0.05	1.0506E-02	1.0973E-01
0.01	-1.65	2.0924E-16	1.8688E-15	0.37	0.10	2.3978E-02	1.4282E-01
0.02	-1.60	4.1848E-16	2.0622E-15	0.38	0.15	4.3259E-02	1.9679E-01
0.03	-1.55	6.2772E-16	2.2555E-15	0.39	0.19	6.2863E-02	2.7687E-01
0.04	-1.50	8.3696E-16	2.4489E-15	0.40	0.24	7.9100E-02	3.8310E-01
0.05	-1.45	1.0462E-15	2.6422E-15	0.41	0.29	9.5539E-02	5.0814E-01
0.06	-1.41	1.2554E-15	2.8356E-15	0.42	0.34	1.2068E-01	6.3823E-01
0.07	-1.36	1.4647E-15	3.0290E-15	0.43	0.39	1.6410E-01	7.5736E-01
0.08	-1.31	1.6739E-15	3.2223E-15	0.44	0.44	2.3393E-01	8.5309E-01
0.09	-1.26	1.8832E-15	3.4157E-15	0.45	0.48	3.3371E-01	9.2036E-01
0.10	-1.21	2.0924E-15	3.6090E-15	0.46	0.53	4.5893E-01	9.6161E-01
0.11	-1.16	2.3016E-15	3.8024E-15	0.47	0.58	5.9615E-01	9.8363E-01
0.12	-1.11	2.5109E-15	2.8601E-14	0.48	0.63	7.2682E-01	9.9385E-01
0.13	-1.07	2.7201E-15	2.3645E-13	0.49	0.68	8.3454E-01	9.9797E-01
0.14	-1.02	2.9294E-15	1.6225E-12	0.50	0.73	9.1117E-01	9.9941E-01
0.15	-0.97	3.1386E-15	9.7686E-12	0.51	0.78	9.5806E-01	9.9985E-01
0.16	-0.92	3.3478E-15	5.2952E-11	0.52	0.82	9.8270E-01	9.9997E-01
0.17	-0.87	3.5571E-15	2.6233E-10	0.53	0.87	9.9379E-01	9.9999E-01
0.18	-0.82	3.7663E-15	1.2513E-09	0.54	0.92	9.9807E-01	1.0000E+00
0.19	-0.78	2.1733E-14	6.9107E-09	0.55	0.97	9.9948E-01	1.0000E+00
0.20	-0.73	2.1209E-13	2.6769E-08	0.56	1.02	9.9988E-01	1.0000E+00
0.21	-0.68	1.7358E-12	1.1600E-07	0.57	1.07	9.9998E-01	1.0000E+00
0.22	-0.63	1.1373E-11	4.8126E-07	0.58	1.11	1.0000E+00	1.0000E+00
0.23	-0.58	6.4625E-11	1.9316E-06	0.59	1.16	1.0000E+00	1.0000E+00
0.24	-0.53	4.1126E-10	7.5246E-06	0.60	1.21	1.0000E+00	1.0000E+00
0.25	-0.48	2.4773E-09	2.8566E-05	0.61	1.26	1.0000E+00	1.0000E+00
0.26	-0.44	1.2132E-08	1.0566E-04	0.62	1.31	1.0000E+00	1.0000E+00
0.27	-0.39	5.2343E-08	3.7635E-04	0.63	1.36	1.0000E+00	1.0000E+00
0.28	-0.34	2.4478E-07	1.2625E-03	0.64	1.41	1.0000E+00	1.0000E+00
0.29	-0.29	1.0945E-06	3.8474E-03	0.65	1.45	1.0000E+00	1.0000E+00
0.30	-0.24	4.7123E-06	1.0185E-02	0.66	1.50	1.0000E+00	1.0000E+00
0.31	-0.19	1.9709E-05	2.2466E-02	0.67	1.55	1.0000E+00	1.0000E+00
0.32	-0.15	7.9860E-05	4.0237E-02	0.68	1.60	1.0000E+00	1.0000E+00
0.33	-0.10	3.1104E-04	5.9110E-02	0.69	1.65	1.0000E+00	1.0000E+00
0.34	-0.05	1.1366E-03	7.5125E-02	0.70	1.70	1.0000E+00	1.0000E+00
0.35	0.00	3.7379E-03	8.9858E-02	—	—	—	—

NOTE: The mean for true strain is 0.35, shown in bold. The standard deviation (std) of true strain is 0.21.

Source: Ref. D4.1.27, Table 6.3.7.3-1

The weldment at best can have the same mechanical properties as the hosting metal (native metal), but it is usually more brittle than the hosting metal. The failure likelihood of the weldment substructure was considered, reflecting weighting factors of both 1.0 and 0.75 applied to estimated true strain at failure.

The capacity function is based on coupon tensile strength tests in uniaxial tension. However, cracking of a stainless steel may not be determined simply by comparing the calculated plastic strain to the true strain of failure, because the equivalent (or effective) plastic strain (EPS) is calculated from a complex 3-D state of stress, while the true strain at failure was based on data from a 1-D state of stress. A 3-D state of stress may constrain plastic flow in the material and lower the EPS at which failure occurs. This loss of ductility is accounted for by the use of a triaxiality factor, which is the ratio of normal stress to shear stress on the octahedral plane, normalized to unity for simple tension. For the purpose of determining the probability of structural failure, LLNL (Ref. D4.1.27) set the ductility ratio to 0.5. This is equivalent to a triaxiality factor of 2, which corresponds to a state of biaxial tension.

Failure of containment can occur when strain in a component is of sufficient magnitude that it results in breakage or puncture of the container. The probability of failure is calculated based on the maximum strain for a single finite element brick obtained from LS-DYNA simulations. Fracture propagation takes place on the milliseconds time-scale and thus propagates across the canister wall thickness very quickly, compared to the time-frame of the LS-DYNA simulations. Furthermore, the fragility curve is obtained on the basis of a maximum average strain over the thickness of the respective specimens, which are 2-inch-long stainless steel 304L specimens. Although LS-DYNA results provide multiple values of the strain through the thickness of the canister wall (the wall thickness being represented by multiple finite element layers), it is more conservative to use the maximum strain value at a single finite element brick than the average of the multiple values across the thickness of the wall.

The probability of failure for each impact scenario is evaluated by finding the maximum strain at a location in which a through-wall crack would constitute a radionuclide release. A probability of failure is determined from the cumulative distribution function of capacity or fragility curve (as discussed below) from the global maximum strain. |

A conservative approach and aid to computational efficiency is achieved by performing calculations focusing on the regions of the container having high strain (and deformation) after a drop (“hot zones”). An importance sampling strategy was used which places greater-than-random emphasis on ranges of input-variable values, and/or on combinations of such value ranges, that are more likely to affect output. This approach is an alternative to Monte Carlo methods with the important advantage that possible combinations of upper-bound variable values are in fact incorporated into each probabilistic estimate of expected model output (which is not always guaranteed by uniform sampling).

Using the general probabilistic approach summarized here, LLNL (Ref. D4.1.27) calculated failure probabilities for representative canisters in an aging overpack, and in a transportation cask, and for the representative canister itself, as presented in Tables D1.2-2 through D1.2-5. For the drop of a 10-metric-ton load onto a cask, the falling mass is modeled as a rigid (unyielding) wall, oriented normal to longitudinal axis of the cask.

D1.2 IDAHO NATIONAL LABORATORY ANALYSIS OF SPENT NUCLEAR FUEL CANISTERS AND MULTICANISTER OVERPACKS

Drop tests of prototype canisters conducted by the Idaho National Laboratory (INL) confirmed that the stainless steel shell material can undergo significant strains without material failure leading to loss of containment. These drop tests also validated analytical models used to predict strains under various drop scenarios. Table D1.2-6 shows scenarios selected to address potential drop scenarios at YMP facilities and the predicted strains.

INL performed FEA (using ABAQUS/Explicit, which, like LS-DYNA, has been used in nuclear facility and non-nuclear industrial applications, and is appropriate to model nonlinear, transient responses of a passive component to a structural challenge such as a drop or an impact) of 23-foot drops, three degrees off vertical, to determine the extent of strain at various positions in the bottom head, cylindrical shell, and joining weld. The strain was evaluated and reported for the inside, outside, and middle layers (Ref. D4.1.64). The DOE standardized SNF canisters were modeled at 300°F, the maximum skin temperature expected due to the heat evolved by the fuel (based on review of thermal analyses performed by transportation casks vendors), resulting in diminished casing material strength. It was found that greater strains would be expected in the MCOs at ambient temperatures than at elevated temperatures.

During a canister drop event, the majority of the kinetic energy at impact performs work on the material, which causes the worst locations to exhibit plastic strain. A good measure of this work is equivalent plastic strain, which is a cumulative strain measure that takes into account the deformation history starting at impact. From the peak equivalent plastic strain, LLNL (Ref. D4.1.27) developed failure probabilities using the method described in Section D1.1 for an 18 in. and 24 in. DOE standard canister and an MCO. Results are summarized in Table D1.2-7.

Table D1.2-1. Container Configurations and Loading Conditions

Container	Configuration	Drop Type/Impact Condition ^a	Drop Height
AO (aging overpack) cell with canister inside	Representative canister inside AO	A IC 1: End with vertical orientation	3-ft vertical
		A IC 2: Slapdown from a vertical orientation and 2.5 mph horizontal velocity	0-ft vertical
Transportation cask with spent nuclear fuel (SNF) canister inside	Representative canister inside representative cask	T IC 1a: End, with 4 degree off-vertical orientation	12-ft vertical
		T.IC 1b: Same as T.IC 1a	13.1-ft vertical
		T.IC 1c: Same as T.IC 1a	30-ft vertical
		T IC 2a: End, with 4 degree off-vertical orientation, and approximated slapdown	13.1-ft vertical
		T.IC 2b: Same as T.IC 2a, with no free fall	0-ft vertical
		T IC 3: Side, with 3 degree off-horizontal orientation	6-ft vertical
DPC (dual-purpose canister) TAD (transportation, aging, and disposal) canister	Representative canister	D IC 1a: End, with vertical orientation	32.5-ft vertical
		D IC 1b: Same as D.IC 1a	40-ft vertical
		D IC 2a: End, with 4 degree off-vertical orientation	23-ft vertical
		D IC 2b: Same as D.IC 2a	10-ft vertical
		D IC 2c: Same as D.IC 2a	5-ft vertical
		D IC 3: 40 ft/min horizontal collision inside the CTM bell	No drop
		D IC 4: Drop of 10-metric-ton load onto top of canister	10-ft vertical
		D.IC 2a: Hourglass-control study for end drop, with 4 degree off-vertical orientation	23-ft vertical
		D.IC 2a: Friction coefficient sensitivity study for end drop, with 4 degree off-vertical orientation	23-ft vertical
		D.IC 2a: Mesh density study for end drop, with 4 degree off-vertical orientation	23-ft vertical
DSNF (DOE spent nuclear fuel) canister	INL-analyzed case	O.IC 1: End, with 3-degree-off vertical orientation	23-ft vertical

NOTE: A = aging overpack (AO); D = dual-purpose canister; ft = foot; IC = impact condition; min = minute; mph = miles per hour; O = DOE SNF canister; SNF = spent nuclear fuel; T = transportation cask.

Source: ^a Ref. D4.1.27, Table 4.3.3-1a

Table D1.2-2. Failure Probabilities with and without Triaxiality Factor, with and without the Fragility Curve Adjustment, for Representative Canister within an Aging Overpack

Container Type/ Impact Condition ^a	Impact Condition Description	Max EPS ^b	Failure Probability ^b			
			Original CDF Fragility Curve w/o Adjustment		CDF Fragility Curve Adjusted for Minimum Elongation (-8.3% Shift)	
			w/o Triaxiality	w/ Triaxiality	w/o Triaxiality	w/ Triaxiality
A.IC 1	3-ft end drop, with vertical orientation	0.16%	$<1 \times 10^{-8}$	$<1 \times 10^{-8}$	$<1 \times 10^{-8}$	$<1 \times 10^{-8}$
A.IC 2	Slapdown from a vertical orientation and 2.5-mph horizontal velocity	0.82%	$<1 \times 10^{-8}$	$<1 \times 10^{-8}$	$<1 \times 10^{-8}$	$<1 \times 10^{-8}$

NOTE: ^a“A” stands for aging overpack. “IC” stands for impact condition, which are defined in Table D1.2-1.
^bValues of Max EPS and failure probability are applicable to the SNF canister.

Source: Ref. D4.1.27, Table 6.3.7.6-1